A Generalized Framework Towards Structural Mechanics of Three-layered Composite Structures

Marcus Aßmus[1]⋆, Konstantin Naumenko[1], Andreas Öchsner[2], Victor A. Eremeyev[3], Holm Altenbach[1]

[1] Otto von Guericke University, Faculty of Mechanical Engineering, Universitätsplatz 2, 39108 Magdeburg, Germany

[2] Esslingen University of Applied Sciences, Faculty Mechanical Engineering, Kanalstraße 33, 73728 Esslingen, Germany

[3] Gdańsk University of Technology, Faculty of Civil and Environmental Engineering, Narutowicza 11/12, 80-233 Gdańsk, Poland

Abstract: Three-layered composite structures find a broad application. Increasingly, composites are being used whose layer thicknesses and material properties diverge strongly. In the perspective of structural mechanics, classical approaches to analysis fail at such extraordinary composites. Therefore, emphasis of the present approach is on arbitrary transverse shear rigidities and structural thicknesses of the individual layers. Therewith we employ a layer-wise approach for multiple (quasi-)homogeneous layers. Every layer is considered separately whereby this disquisition is based on the direct approach for deformable directed surfaces. We limit our considerations to geometrical and physical linearity. In this simple and familiar setting we furnish a layer-wise theory by introducing constraints at interfaces to couple the layers. Hereby we restrict our concern to surfaces where all material points per surface are coplanar and all surfaces are plane parallel. Closed-form solutions of the governing equations enforce a narrow frame since they are strongly restrictive in the context of available boundary conditions. Thus a computational solution approach is introduced using the finite element method. In order to determine the required spatially approximated equation of motion, the principle of virtual work is exploited. The discretization is realized via quadrilateral elements with quadratic shape functions. Hereby we introduce an approach where nine degrees of freedom per node are used. In combination with the numerical solution approach, this layer-wise theory has emerged as a powerful tool to analyze composite structures. In present treatise, we would like to clarify the broad scope of this approach.

Keywords: general composite structure, high contrast plates, generalized approach, layer-wise theory

1 Introduction

1.1 Motivation

Nowadays, composite structures are applied in a wide range of applications. Composites with unusual and unique properties are becoming more and more important. This statement refers to the fact that composites are increasingly being developed which consist of a broad spectrum of mechanical and geometrical properties. The definition of a composite structure in the context of thin-walled structural elements is primarily defined by its geometry, i.e. lengths L_α and layer thicknesses h^K while K is a layer index.

$$L_\alpha \gg H \qquad\qquad H = \sum_K^{NK} h^K \qquad\qquad (1)$$

In general, the number of layers of the composite NK is arbitrary. However, we restrict our concern to composite structures with three layers (NK = 3). Up to now, classifications for composite structures are missing. Main representatives of this genus are depicted in Fig. 1. This subdivision is sufficient at least for engineering applications. The symmetry of the structural design depicted there is not a compelling limitation. Certainly there are other special cases. However, we can distinguish three kinds of three-layered composite structures (TLCS). Theses are laminates, sandwiches, and anti-sandwiches. They can be distinguished by typical geometric and material relationships. Sandwiches and anti-sandwiches exhibit shear-deformable core layers while the skin layers are shear-rigid. Conspicuously, sandwiches and anti-sandwiches are geometrically contrary. Laminates, on the other hand, have similar layer thicknesses and the material properties are all in the same order of magnitude.

Several theories for the treatment of mechanical problems at such composite structures exist. Thereby we reduce our perspective to the efficient and elegant treatment by means of theories for thin walled-structures, cf. Naghdi (1972). A comprehensive view at thin-walled structural elements incorporating historical remarks on relevant protagonists is given in Altenbach and Eremeyev (2017). In Carrera (2002, 2003), basic approaches to treat composite structures are discussed whereby it is distinguished between *equivalent single layer models* and *layer-wise models*. For the former, the *classical laminate theory* and *first-order shear deformation theory* are prominent instances. These modeling approaches are predominantly suitable for monocoque structures (single-layered, homogeneous, isotropic). Another acquaintance is the *sandwich theory*. However, these approaches fail when focusing on strongly divergent material properties and structural thicknesses. There are many theoretical approaches to this, but most of them are only suitable for special compositions and thus have only a limited scope of application. Therefore, a
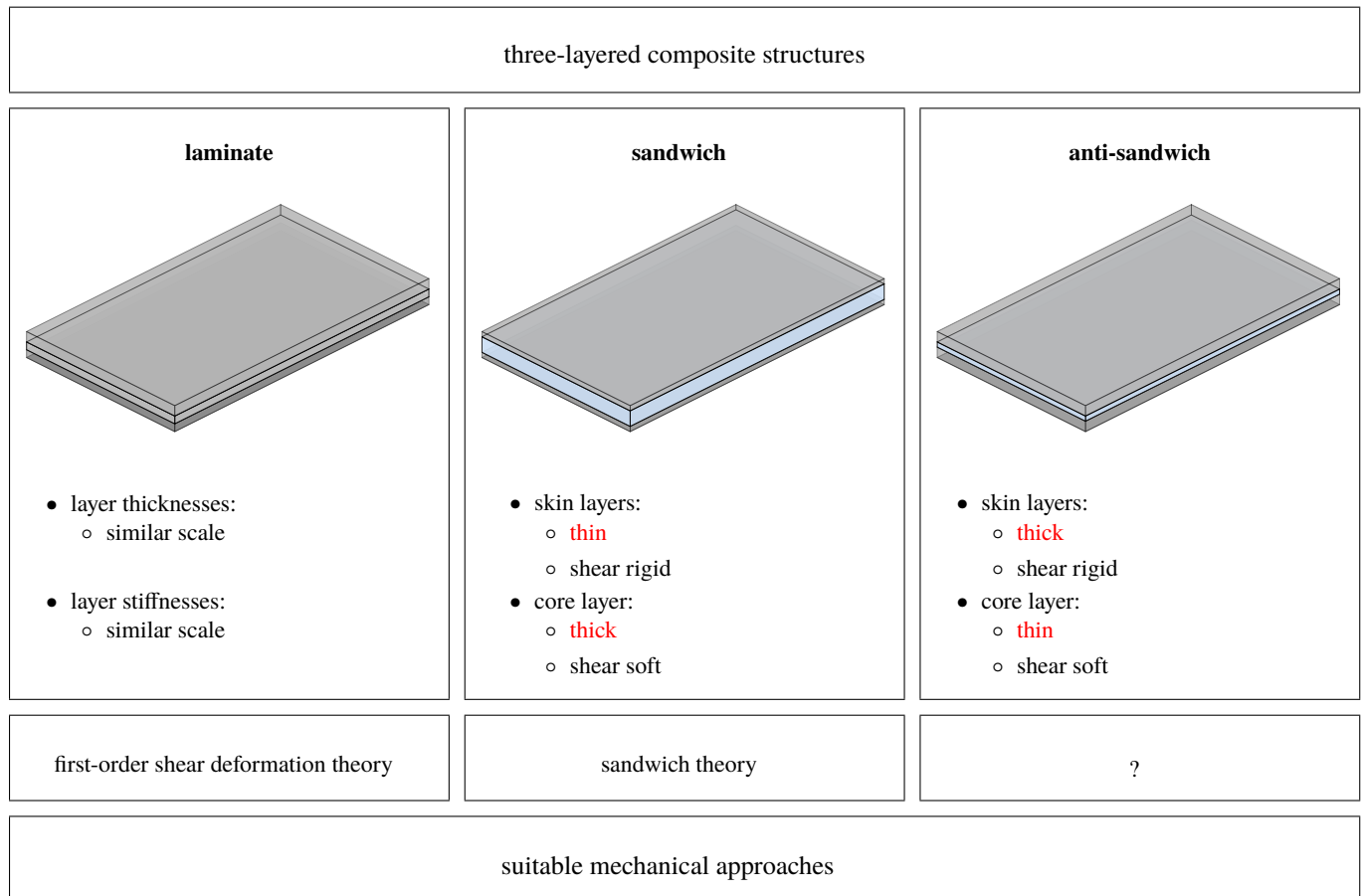
Fig. 1: Attempt of a general classification of three-layered composite structures used for applications in engineering sciences

generalized approach for a wide range of applications is of interest. Present treatise is dedicated to a generalized framework to handle structural mechanics problems at TLCS. For this, we introduce the so called *eXtended layer-wise theory* (XLWT) which also provides a very efficient solution approach for a wide range of mechanical problems in present genus.

1.2 Structure

In order to give our representation an easily readable and condensed shape, we make use of the direct tensor notation. Therefore, we explain present notational conventions and recapitulate the basics of tensor calculus before starting with the actual executions. After that, we will directly enter into the main features of our approach. In doing so, we follow the executions presented in Naumenko and Eremeyev (2014). This base is enlarged since we consider arbitrary transverse shear stiffnesses for all three layers. Thereby we follow a procedure called *direct approach* in spirit of Cosserat and Cosserat (1909), cf. Ganghoffer (2017). We operate on a deformable directed surface *ab initio*. This is a surface in the three-dimensional space in which a vector field is additionally assigned to each point (Zhilin, 1976). We introduce this surface as primitive concept, i.e. it is just an illustrative mean for the stretching, shearing, bending, and twisting of a single layer. However, in present context we introduce the restriction that all material points of this two-dimensional subset are coplanar, i.e. our surface is initially non-curved. In contrast to *derived approaches* where a hierarchic procedure for the derivation of two-dimensional balance equations and kinematic relations is presented, cf. Naghdi (1972), we are liberated from such purely pragmatic approaches, as they are usually applied in engineering sciences (Libai and Simmonds, 1983). This is why the attribute *geometrically exact* is often used in literature.

In progress, we embed the *direct approach* in a systematic framework to establish a layer-wise theory. Thereby, three surfaces are stacked plane parallel equidistantly whereby interfaces and outer faces are initiated for physical reasons. After introducing constraints, the governing equations of the composite structure are derived by the aid of global variables. These equations remain valid for arbitrary structural thicknesses and material parameters.

To construct approximate solutions we make us of the calculus of variations and exploit the principle of virtual work. Subsequently, a numerical method by the aid of the finite element method (FEM) is introduced to solve the algebraic form of the partial differential equations of the boundary value problem.

This is followed by a detailed analysis of the range of application whereby we reduce our investigations to symmetric composites for the sake of brevity. In particular, the roles of different transverse geometry and material compositions are discussed in some detail. As a central result, it is shown that the present approach spans a broad application range at least in context of engineering applications. Finally, the basic findings are summarized and relevant conclusions are drawn. In order to provide users with a complete tool for solving problems with three-layered composites, supplementary relevant matrices like constitutive quantities and differential operators are collected in the Appendix.

Notation. Throughout the whole text, a direct tensor notation is preferred. First- and second-order tensors are denoted by lowercase and uppercase bold letters, e.g., a and A, respectively. Fourth-order tensors are designated by uppercase blackboard bold letters, e.g. $\mathbb{A}$. In continuation, some operations between these tensors need to be defined which will be done based on a Cartesian coordinate system. These operations are the dyadic product

$$a \otimes b = a_i b_j e_i \otimes e_j = C, \tag{2}$$

the scalar product

$$a \cdot b = a_i b_j e_i \cdot e_j = a_i b_i = \alpha, \tag{3}$$

the composition of a second and a first order tensor

$$A \cdot a = A_{lm} a_i e_l \otimes e_m \cdot e_i = A_{li} a_i e_l = d, \tag{4}$$

the double scalar product between a fourth and a second order tensor

$$\mathbb{A} : B = A_{pqrs} B_{no} e_p \otimes e_q \otimes e_r \otimes e_s : e_n \otimes e_o = A_{pqrs} B_{sr} e_p \otimes e_q = D, \tag{5}$$

the double scalar product between two fourth-order tensors

$$\mathbb{A} : \mathbb{B} = A_{pqrs} B_{tuvw} e_p \otimes e_q \otimes e_r \otimes e_s : e_t \otimes e_u \otimes e_v \otimes e_w = A_{pqrs} B_{srvw} e_p \otimes e_q \otimes e_v \otimes e_w = \mathbb{F}, \tag{6}$$

the cross product between tow first-order tensors

$$a \times b = a_i b_j e_i \times e_j = a_i b_j \epsilon_{ijk} e_k = c, \tag{7}$$

the cross product between a second and a first-order tensor

$$A \times b = A_{lm} b_j e_l \otimes e_m \times e_j = A_{lm} b_j \epsilon_{mjk} e_l \otimes e_k = J. \tag{8}$$

Herein we have introduced the Levi-Civita symbol ϵ_{ijk}.

$$\epsilon_{ijk} = -^1/_2 (j - i)(k - j)(i - k) \tag{9}$$

The inverse of a tensor is defined by

$$A^{-1} \cdot A = A \cdot A^{-1} = 1 \qquad\qquad \left[A^{-1} \right]^{-1} = A \tag{10}$$

while the transposed of a tensor is given by

$$a \cdot A^\top \cdot b = b \cdot A \cdot a. \tag{11}$$

Herein, $1 = e_i \otimes e_i$ is the identity on first order tensors. A tensor is said to be symmetric if $A^\top = A$ holds. The nabla operator is defined as $\boldsymbol{\nabla} = e_i \partial/\partial x_i$ for three‐dimensional considerations. $\boldsymbol{\nabla} \cdot \square$ and $\boldsymbol{\nabla}\square$ is the gradient of a tensor, where $\square$ holds true for every differentiable tensor field. The transposed gradient is defined as $\boldsymbol{\nabla}^\top \square = [\boldsymbol{\nabla}\square]^\top$, and $\boldsymbol{\nabla}^{\mathrm{sym}}\square = {}^1/_2 \left[\boldsymbol{\nabla}\square + \boldsymbol{\nabla}^\top\square \right]^\top$ is the symmetric part of the corresponding gradient, where $\square$ holds for all first‐order tensors. However, in protruding introduction we have used latin indices, e.g. $i \in \{1, 2, 3\}$. The application of greek indices such as $\alpha \in \{1, 2\}$ applies analogously. A subscript zero refers to the reference placement of the material body manifold and a superscript star is used to designate prescribed quantities at boundaries. Material body manifolds are denoted by letters in gothic print (e.g. $\mathfrak{S}$ or $\mathfrak{R}$). For numerical vectors and matrices we make use of upright, sans-serif, lowercase and uppercase bold letters, e.g., a and A, respectively.

2 Background

2.1 Theoretical Approach

As mentioned at the beginning, we follow the *direct approach*, i.e. we start operating on two-dimensional body manifolds *ab initio*. We introduce mid-surfaces $\mathfrak{S}^K$ for all three layers of the composite structure considered, namely the top layer (index t), the core layer (index c), and the bottom layer (index b). Nonetheless, our model is based on three-dimensional body manifolds so that every physical layer occupies the region $\mathfrak{S}^K \times [-^{h^K}/_2, {}^{h^K}/_2]$ whereby we assume uniform layer thicknesses. Herein we use $K = \{t, c, b\}$ as layer index. The surface $\mathfrak{S}^K$ is endowed with an orthonormal coordinate system $\{e_\alpha, n\}$. Every surface is spanned by a two-dimensional position vector $r^K = X_\alpha^K e_\alpha$, i.e. all material points are coplanar. The parameters $X_\alpha^K \ \forall \alpha = \{1, 2\}$ are the coordinates of the corresponding surface.

Additionally, interfaces $\mathfrak{I}^K$ between the layers are used while the outer surfaces $\mathfrak{O}$ (front) and $\mathfrak{B}$ (back) are cultivated as load application areas. All surfaces, and thus also all interfaces as well as both outer surfaces are plane-parallel. The distance of the surface $\mathfrak{S}^K$ to the interfaces $\mathfrak{I}^K$ or respectively to the outer surface $\mathfrak{O}$ and $\mathfrak{B}$ is $\mp^{h^K}/_2$. The origin of the global coordinate system for present composite structure is set at $\mathfrak{S}^c$ concerning the transverse direction so that $-h^t - {}^{h^c}/_2 \leq X_3 \leq {}^{h^c}/_2 + h^b$ holds, cf. Fig. 2.
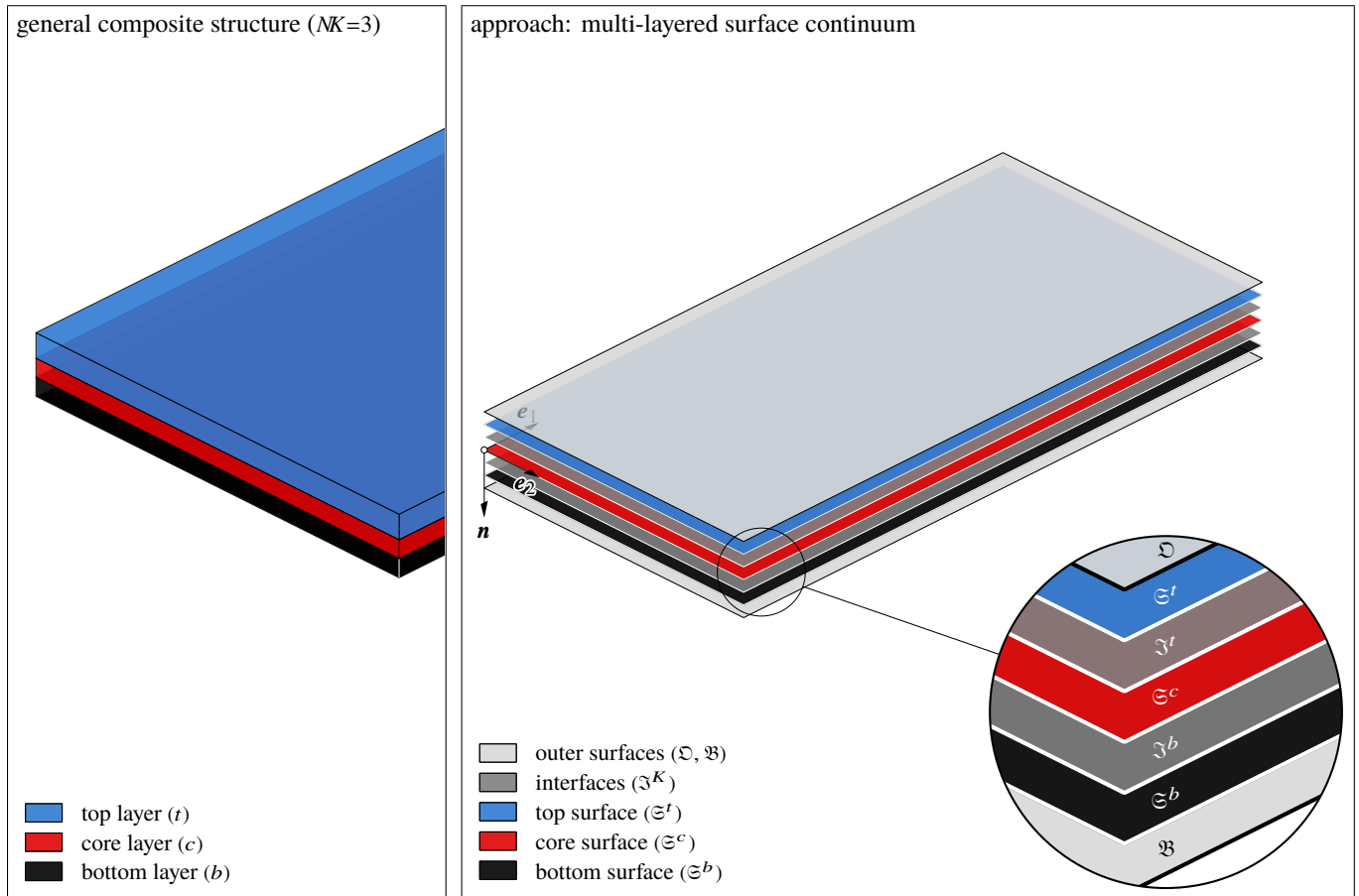
Fig. 2: General composite structure and theoretical considerations restricted to individual surfaces and interfaces

2.1.1 Kinematics

We are dealing with a five-parameter theory, i.e. every surface features three translational and two rotational degrees of freedom. These are summarized in the vectors of translations $\boldsymbol{a}$ and of rotations $\boldsymbol{\varphi}$.

$$\boldsymbol{a}^K = \boldsymbol{v}^K + w^K \boldsymbol{n} \qquad \text{with } \boldsymbol{v}^K = v_\alpha^K \boldsymbol{e}_\alpha \tag{12a}$$

$$\boldsymbol{\varphi}^K = \varphi_\alpha^K \boldsymbol{e}_\alpha \tag{12b}$$

In contrast to a Cosserat surface (with $\boldsymbol{\varphi} = \varphi_\alpha \boldsymbol{e}_\alpha + \varphi_3 \boldsymbol{n} \ \forall i \in \{1,2,3\}$) we neglect drilling rotations φ_3. This is justified since the resistance against wrinkling is much higher compared to that of bending, which is however a pragmatic approach, as is typical in engineering sciences. We furthermore introduce a more physical rotation vector $\boldsymbol{\psi} = -\varphi_2 \boldsymbol{e}_1 + \varphi_1 \boldsymbol{e}_2$ in the spirit of Mindlin (1951), related to the one introduced in Eq. (12b) by $\boldsymbol{\varphi} = \boldsymbol{\psi} \times \boldsymbol{n}$. Based on the degrees of freedoms utilised here, the following special set of deformation measures emerges.

$$\boldsymbol{G}^K = \boldsymbol{\nabla}^{\text{sym}} \boldsymbol{v}^K \tag{13a}$$

$$\boldsymbol{K}^K = \boldsymbol{\nabla}^{\text{sym}} \boldsymbol{\varphi}^K \tag{13b}$$

$$\boldsymbol{g}^K = \boldsymbol{\nabla} w^K + \boldsymbol{\varphi}^K \tag{13c}$$

Here, $\boldsymbol{G}^K = G_{\alpha\beta}^K \boldsymbol{e}_\alpha \otimes \boldsymbol{e}_\beta$ is the in-plane strain tensor, $\boldsymbol{K}^K = K_{\alpha\beta}^K \boldsymbol{e}_\alpha \otimes \boldsymbol{e}_\beta$ is the curvature change tensor, and $\boldsymbol{g}^K = g_\alpha^K \boldsymbol{e}_\alpha$ is the transverse shear strain vector.

2.1.2 Kinetics

Boundary quantities are defined by forces and moments acting at the surface which is in analogy of Cauchys theorem (Cauchy, 2009). Thereby we introduce tangential forces $s_\mathfrak{S}^K$ and orthogonal forces $p_\mathfrak{S}^K$, as well as out-of-plane moments $\boldsymbol{m}_\mathfrak{S}^K$ acting at every single surface.

$$\boldsymbol{n}_{\boldsymbol{\nu}}^K = \lim_{\Delta L \to 0} \frac{\Delta s_\mathfrak{S}^K}{\Delta L} \qquad \boldsymbol{m}_{\boldsymbol{\nu}}^K = \lim_{\Delta L \to 0} \frac{\Delta(\boldsymbol{m}_\mathfrak{S}^K \times \boldsymbol{n})}{\Delta L} \qquad q_{\boldsymbol{\nu}}^K = \lim_{\Delta L \to 0} \frac{\Delta p_\mathfrak{S}^K}{\Delta L} \tag{14}$$

Herein L is a length measure. The vectors and the scalar of the left hand-sides indicate the boundary resultants of the in-plane state $\boldsymbol{n}_{\boldsymbol{\nu}}^K$, the out-of-plane state $\boldsymbol{m}_{\boldsymbol{\nu}}^K$ and the transverse shear state $q_{\boldsymbol{\nu}}^K$. The orientation of the cut is defined by the corresponding

normal. Thereby we make use of the boundary normals $\boldsymbol{n}$ and $\boldsymbol{\nu}$, whereby $\boldsymbol{n} \cdot \boldsymbol{\nu} = 0$ holds. Following Cauchy, a tensor field exists to the boundary resultants introduced in Eq. (14). The following applies to boundaries with normals $\boldsymbol{n}$.

$$\boldsymbol{n} \cdot \boldsymbol{N}^K = \mathbf{o} \qquad\qquad \boldsymbol{n} \cdot \boldsymbol{L}^K = \mathbf{o} \qquad\qquad \boldsymbol{n} \cdot \boldsymbol{q}^K = 0 \tag{15}$$

However, with the boundary normal $\boldsymbol{\nu}$, which points along the plane directions, the following boundary loads result.

$$\boldsymbol{\nu} \cdot \boldsymbol{N}^K = \boldsymbol{n}_{\boldsymbol{\nu}}^K \qquad\qquad \boldsymbol{\nu} \cdot \boldsymbol{L}^K = \boldsymbol{m}_{\boldsymbol{\nu}}^K \qquad\qquad \boldsymbol{\nu} \cdot \boldsymbol{q}^K = q_{\boldsymbol{\nu}}^K \tag{16}$$

Analogous to Cauchys Lemma, the resultants at opposite edges are equal in magnitude, but antithetically.

$$\boldsymbol{n}_{\boldsymbol{\nu}}^K(-\boldsymbol{\nu}) = -\boldsymbol{n}_{\boldsymbol{\nu}}^K(\boldsymbol{\nu}) \qquad\qquad \boldsymbol{m}_{\boldsymbol{\nu}}^K(-\boldsymbol{\nu}) = -\boldsymbol{m}_{\boldsymbol{\nu}}^K(\boldsymbol{\nu}) \qquad\qquad q_{\boldsymbol{\nu}}^K(-\boldsymbol{\nu}) = -q_{\boldsymbol{\nu}}^K(\boldsymbol{\nu}) \tag{17}$$

Tensors for the stress resultants arise from Eqs. (15) and (16). Here $\boldsymbol{N}^K = N_{\alpha\beta}^K \boldsymbol{e}_\alpha \otimes \boldsymbol{e}_\beta$ is the in-plane force tensor, $\boldsymbol{L}^K = M_{\alpha\beta}^K \boldsymbol{e}_\alpha \otimes \boldsymbol{e}_\beta$ is the polar tensor of moments, and $\boldsymbol{q}^K = Q_\alpha^K \boldsymbol{e}_\alpha$ is the transverse shear force vector.

2.1.3 Constitutive Relations

We reduce our concern to homogeneous and isotropic materials and consider a simple elastic material in the spirit of Noll (1958), where the kinetics in maximum depend on the first gradient of the deformation measures. Since we consider decoupled deformations states, the dependencies can be given by the mappings $\mathcal{F}_i^K$ being constitutive functions.

membrane state: $\qquad \boldsymbol{N}^K = \mathcal{F}_1^K\left(\boldsymbol{G}^K\right) \tag{18a}$

bending state: $\qquad \boldsymbol{L}^K = \mathcal{F}_2^K\left(\boldsymbol{K}^K\right) \tag{18b}$

transverse shear state: $\boldsymbol{q}^K = \mathcal{F}_3^K\left(\boldsymbol{g}^K\right) \tag{18c}$

When linearizing the functions $\mathcal{F}_i^K$, which is justified in a completely linear theory, we can determine the following constitutive tensors (Aßmus et al., 2017b).

$$\mathcal{F}_1^K: \quad \mathbb{A}^K = 2B^K h^K \quad \mathbb{P}_1 + 2G^K h^K \quad \mathbb{P}_2 \tag{19a}$$

$$\mathcal{F}_2^K: \quad \mathbb{D}^K = 2B^K \frac{\left(h^K\right)^3}{12} \mathbb{P}_1 + 2G^K \frac{\left(h^K\right)^3}{12} \mathbb{P}_2 \tag{19b}$$

$$\mathcal{F}_3^K: \quad \boldsymbol{Z}^K = 2G^K \frac{\kappa^K h^K}{2} \boldsymbol{P} \tag{19c}$$

We thereby make use of the projector representation which allows a clear split into dilatoric and deviatoric portions (Rychlewski, 1984). The fourth-order tensors $\mathbb{P}_\alpha$ and the second-order tensor $\boldsymbol{P}$ used therein are defined as follows.

$$\mathbb{P}_1 = {}^1\!/\!{}_2\, \boldsymbol{P} \otimes \boldsymbol{P} \tag{20}$$
$$\mathbb{P}_2 = \mathbb{P}^{\mathrm{sym}} - \mathbb{P}_1 \tag{21}$$
$$\boldsymbol{P} = \boldsymbol{e}_\alpha \otimes \boldsymbol{e}_\alpha \tag{22}$$

Herein, $\boldsymbol{P}$ is the first metric tensor and $\mathbb{P}^{\mathrm{sym}} = {}^1\!/\!{}_2\,(\boldsymbol{e}_\alpha \otimes \boldsymbol{e}_\beta \otimes \boldsymbol{e}_\alpha \otimes \boldsymbol{e}_\beta + \boldsymbol{e}_\alpha \otimes \boldsymbol{e}_\beta \otimes \boldsymbol{e}_\beta \otimes \boldsymbol{e}_\alpha)$ is the symmetric part of the fourth-order identity of a plane surface. In Eqs. (19a)–(19c) we've introduced two material parameters B^K and G^K. This is the compression modulus of the surface $B^K = Y^K/(2-2\nu^K)$ and the shear modulus $G^K = Y^k/(2+\nu^K)$, while Y^k is Young's modulus and ν^K is Poisson's ratio. We furthermore make use of the structural thickness of the individual layer (h^K) and an individual transverse shear correction factor ($0 < \kappa^K \leq 1$, Vlachoutsis (1992)). In order to relate this representation to the ones used in classical theories for thin-walled members, the stiffnesses associated with the individual deformation portions are introduced. These are the membrane stiffness D_{M}^K, the bending stiffness D_{B}^K, and the transverse shear stiffness D_{S}^K, determined by the arithmetic means of the stiffness measures introduced in (19a)–(19c).

$$D_{\mathrm{M}}^K = \frac{1}{2}\left[2B^K h^K \quad +2G^K h^K\right] \tag{23a}$$

$$D_{\mathrm{B}}^K = \frac{1}{2}\left[2B^K \frac{\left(h^K\right)^3}{12} + 2G^K \frac{\left(h^K\right)^3}{12}\right] \tag{23b}$$

$$D_{\mathrm{S}}^K = \kappa^K G^K h^K \tag{23c}$$

By the aid of these engineering stiffnesses, one can reformulate Eqs. (19a)–(19c) to a Lamé-like representation (Lamé, 1866), cf. Aßmus (2019). However, through above procedure we can write the constitutive relations as linear mappings in analogy to Hooke's law (Hooke, 1678).

$$\boldsymbol{N}^K = \mathbb{A}^K : \boldsymbol{G}^K \tag{24a}$$
$$\boldsymbol{L}^K = \mathbb{D}^K : \boldsymbol{K}^K \tag{24b}$$
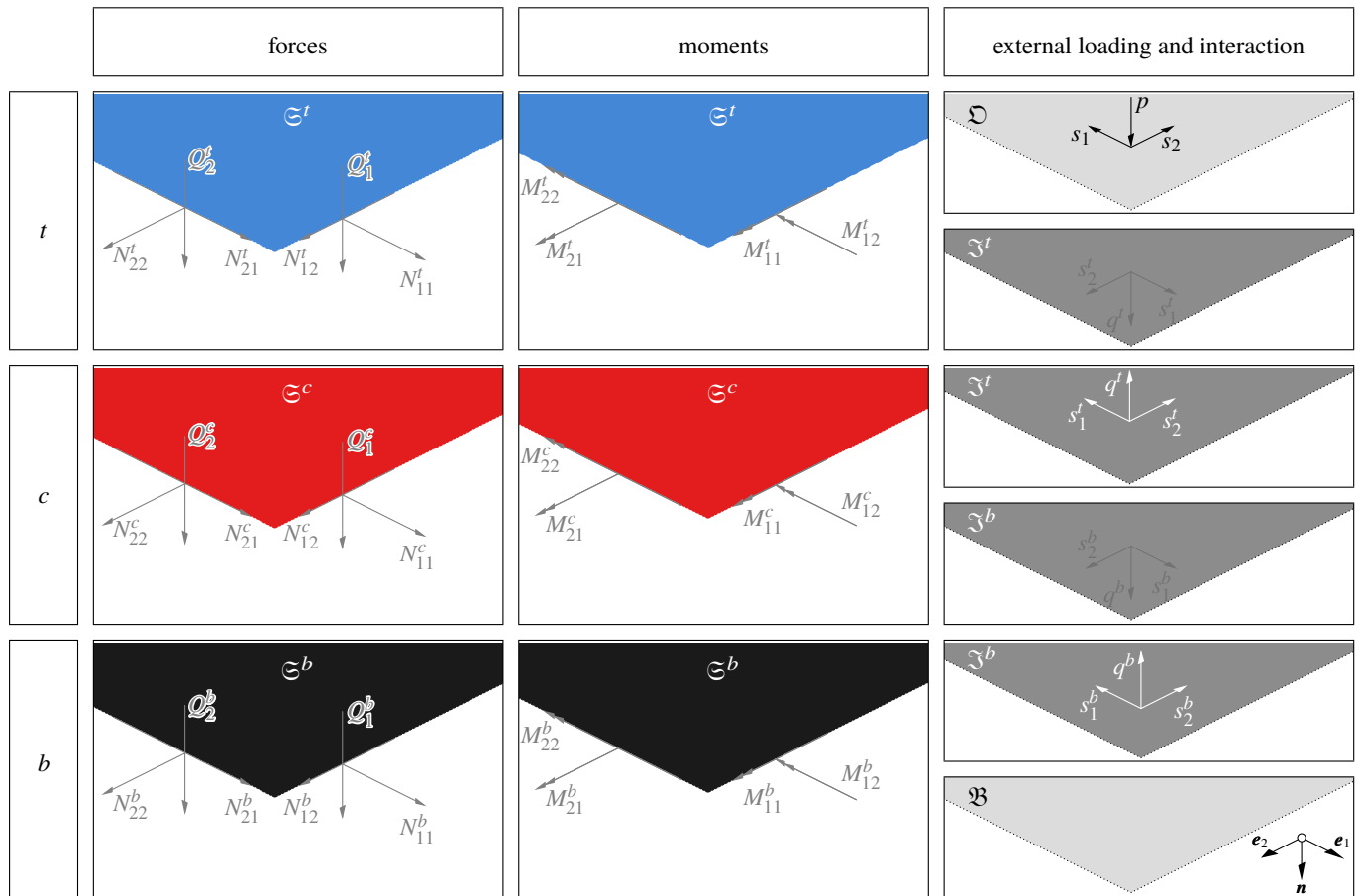$$\boldsymbol{q}^K = \boldsymbol{Z}^K \cdot \boldsymbol{g}^K \tag{24c}$$

Fig. 3: Geometry, material, boundary conditions and discretization to determine the range of application of present approach

2.1.4 Boundary Conditions

For the description of the boundary conditions we distinguish between Dirichlet $\partial\mathfrak{S}_\mathrm{D}$ and Neumann boundaries $\partial\mathfrak{S}_\mathrm{N}$, which are defined at the boundary $\partial\mathfrak{S}$ of every two-dimensional body manifold.

$$\partial\mathfrak{S}^K = \partial\mathfrak{S}^K_\mathrm{D} \cup \partial\mathfrak{S}^K_\mathrm{N} \qquad\qquad\qquad \partial\mathfrak{S}^K_\mathrm{D} \cap \partial\mathfrak{S}^K_\mathrm{N} = \emptyset \qquad\qquad (25)$$

First, we define constraints in the form of prescribed translations and rotations.

$$
\begin{aligned}
\boldsymbol{v}^K(\boldsymbol{r}_0) &= \left(\boldsymbol{v}^K\right)^\star(\boldsymbol{r}_0) \\
\boldsymbol{\varphi}^K(\boldsymbol{r}_0) &= \left(\boldsymbol{\varphi}^K\right)^\star(\boldsymbol{r}_0) \qquad\qquad\qquad \forall\, \boldsymbol{r}_0^K \in \partial\mathfrak{S}_\mathrm{D} \\
w^K(\boldsymbol{r}_0) &= \left(w^K\right)^\star(\boldsymbol{r}_0^K)
\end{aligned}
\qquad (26)
$$

Further, it is possible to link forces and moments that can act as loads at the boundary of the surface continuum with the stress resultants.

$$\boldsymbol{v}\cdot\boldsymbol{N}^K = \left(\boldsymbol{n}_{\boldsymbol{v}}^K\right)^\star \qquad\qquad \boldsymbol{v}\cdot\boldsymbol{L}^K = \left(\boldsymbol{m}_{\boldsymbol{v}}^K\right)^\star \qquad\qquad \boldsymbol{v}\cdot\boldsymbol{q}^K = \left(q_{\boldsymbol{v}}^K\right)^\star \qquad\qquad \forall\, \boldsymbol{r}_0^K \in \partial\mathfrak{S}_\mathrm{N} \qquad (27)$$

2.1.5 Coupling Constraints

In order to couple the three layers whose basic equations have been considered separately up to this point, kinematic constraints are introduced. These are as follows.

- straight line hypothesis (Mindlin, 1951) holds true for every $\mathfrak{S}^K \; \forall\, K \in \{t, c, b\}$ separately
- identical deflections of all layers
- no slipping at interfaces (virgin state)

We use these restrictions to formulate subsequent constraints.

$$\boldsymbol{v}^t + \frac{h^t}{2}\boldsymbol{\psi}^t = \boldsymbol{v}^c - \frac{h^c}{2}\boldsymbol{\psi}^c \qquad\qquad \text{on } \mathfrak{I}^t \tag{28a}$$

$$\boldsymbol{v}^b - \frac{h^b}{2}\boldsymbol{\psi}^b = \boldsymbol{v}^c + \frac{h^c}{2}\boldsymbol{\psi}^c \qquad\qquad \text{on } \mathfrak{I}^b \tag{28b}$$

$$w = w^t = w^c = w^b \qquad\qquad \forall\,\mathfrak{S}^K \tag{28c}$$

By the aid of these simplifications we can reduce the number of independent degrees of freedom to nine, i.e. u_1^t, u_2^t, u_1^b, u_2^b, w, φ_1^t, φ_2^t, φ_1^b, and φ_2^b.

2.1.6   Global Variables

Due to the constraints introduced, the degrees of freedom depend on measures of the top and bottom layer only. That is why we introduce global variables with superscript indexes $^\circ$ and $^\triangle$. These quantities are introduced with respect to the global coordinate system with origin at $-h^t - {}^{h^c}\!/_2 \le X_3 \le {}^{h^c}\!/_2 + h^b$. We inaugurate these global quantities for the degrees of freedom

$$\boldsymbol{v}^\circ = {}^1\!/_2\left[\boldsymbol{v}^t + \boldsymbol{v}^b\right] \qquad\qquad\qquad \boldsymbol{v}^\triangle = {}^1\!/_2\left[\boldsymbol{v}^t - \boldsymbol{v}^b\right] \tag{29a}$$

$$\boldsymbol{\varphi}^\circ = {}^1\!/_2\left[\boldsymbol{\varphi}^t + \boldsymbol{\varphi}^b\right] \qquad\qquad\qquad \boldsymbol{\varphi}^\triangle = {}^1\!/_2\left[\boldsymbol{\varphi}^t - \boldsymbol{\varphi}^b\right], \tag{29b}$$

the deformation measures

$$\boldsymbol{G}^\circ = {}^1\!/_2\left[\boldsymbol{G}^t + \boldsymbol{G}^b\right] \qquad\qquad\qquad \boldsymbol{G}^\triangle = {}^1\!/_2\left[\boldsymbol{G}^t - \boldsymbol{G}^b\right] \tag{30a}$$

$$\boldsymbol{K}^\circ = {}^1\!/_2\left[\boldsymbol{K}^t + \boldsymbol{K}^b\right] \qquad\qquad\qquad \boldsymbol{K}^\triangle = {}^1\!/_2\left[\boldsymbol{K}^t - \boldsymbol{K}^b\right] \tag{30b}$$

$$\boldsymbol{g}^\circ = {}^1\!/_2\left[\boldsymbol{g}^t + \boldsymbol{g}^b\right] \qquad\qquad\qquad \boldsymbol{g}^\triangle = {}^1\!/_2\left[\boldsymbol{g}^t - \boldsymbol{g}^b\right], \tag{30c}$$

the constitutive tensors

$$\mathbb{A}^\circ = \mathbb{A}^t + \mathbb{A}^b \qquad\qquad\qquad\qquad \mathbb{A}^\triangle = \mathbb{A}^t - \mathbb{A}^b \tag{31a}$$

$$\mathbb{D}^\circ = \mathbb{D}^t + \mathbb{D}^b \qquad\qquad\qquad\qquad \mathbb{D}^\triangle = \mathbb{D}^t - \mathbb{D}^b \tag{31b}$$

$$\boldsymbol{Z}^\circ = \boldsymbol{Z}^t + \boldsymbol{Z}^b \qquad\qquad\qquad\qquad \boldsymbol{Z}^\triangle = \boldsymbol{Z}^t - \boldsymbol{Z}^b, \tag{31c}$$

and the stress resultants

$$\boldsymbol{N}^\circ = \sum_K \boldsymbol{N}^K \qquad\qquad\qquad\qquad \boldsymbol{N}^\triangle = \boldsymbol{N}^t - \boldsymbol{N}^b \tag{32a}$$

$$\boldsymbol{L}^\circ = \sum_K \boldsymbol{L}^K + \frac{1}{2}[h^c + h^b]\boldsymbol{N}^b + \frac{1}{2}[h^c + h^t]\boldsymbol{N}^t \qquad\qquad \boldsymbol{L}^\triangle = \boldsymbol{L}^t - \boldsymbol{L}^b \tag{32b}$$

$$\boldsymbol{q}^\circ = \sum_K \boldsymbol{q}^K \qquad\qquad\qquad\qquad \boldsymbol{q}^\triangle = \boldsymbol{q}^t - \boldsymbol{q}^b. \tag{32c}$$

For the sake of simplicity we introduce subsequent abbreviations for geometric measures.

$$h^\circ = {}^1\!/_2\left[h^t + h^b\right] \qquad\qquad\qquad\qquad h^\triangle = {}^1\!/_2\left[h^t - h^b\right] \tag{33a}$$

This helps us to keep the equations in the subsequent procedures as compact as possible. We have to point out that this introduction is arbitrary. As described in Aßmus (2019), all of these global quantities are clearly traceable to layer-wise quantities $K \in \{t, c, b\}$.

2.1.7   Variational Form

As usual, closed-form solutions are feasible for special compositions, boundary conditions, and loading scenarios only. Approaches to such solutions can be found in Naumenko and Eremeyev (2014) (plate strip with shear-rigid skins) or Eisenträger et al. (2015) (plate with shear-rigid skins), for example. A general closed-form solution of the present problem does not exist, which would have to be proven. In contrast to such laborious solution approaches, computational solutions gained huge popularity nowadays. The most popular one seems one seems to be the finite element method Finite Element Method (FEM). The FEM is based on the weak formulation since this relation usually represents a variational principle which is satisfied by the solution. This is achieved here by exploiting the principle of virtual work (PVW). PVW is characterized by the global virtual work balance.

$$\delta W_{\text{int}} = \delta W_{\text{ext}} \tag{34}$$

Considering aforementioned governing equations while involving the global variables introduced, weighting the balance equations with test functions equivalent to the vectors of the degrees of freedom and subsequent partial integration over the area of

investigation $\Re$, we can derive the following expressions for the virtual internal work

$$
\begin{aligned}
\delta W_{\text{int}} = \int_{\Re} \Big\{ \; & \delta \boldsymbol{G}^\circ : \mathbb{A}^\circ : \boldsymbol{G}^\circ + \delta \boldsymbol{G}^\Delta : \mathbb{A}^\circ : \boldsymbol{G}^\Delta + \delta \boldsymbol{G}^\circ : \mathbb{A}^\Delta : \boldsymbol{G}^\Delta \\
& + \delta \boldsymbol{G}^\Delta : \mathbb{A}^\Delta : \boldsymbol{G}^\circ + \left[\delta \boldsymbol{G}^\circ + \tfrac{1}{2} h^\Delta \delta \boldsymbol{K}^\circ + \tfrac{1}{2} h^\circ \delta \boldsymbol{K}^\Delta \right] : \mathbb{A}^c : \left[\boldsymbol{G}^\circ + \tfrac{1}{2} h^\Delta \boldsymbol{K}^\circ + \tfrac{1}{2} h^\circ \boldsymbol{K}^\Delta \right] \\
& + \delta \boldsymbol{g}^\circ \cdot \boldsymbol{Z}^\circ \cdot \boldsymbol{g}^\circ + \delta \boldsymbol{g}^\Delta \cdot \boldsymbol{Z}^\circ \cdot \boldsymbol{g}^\Delta + \delta \boldsymbol{g}^\circ \cdot \boldsymbol{Z}^\Delta \cdot \boldsymbol{g}^\Delta + \delta \boldsymbol{g}^\Delta \cdot \boldsymbol{Z}^\circ \cdot \boldsymbol{g}^\circ \\
& + \left[\delta \boldsymbol{g}^\circ - \tfrac{1}{h^c} \left(2\delta \boldsymbol{v}^\Delta + (h^c + h^\circ) \delta \boldsymbol{\varphi}^\circ + h^\Delta \delta \boldsymbol{\varphi}^\Delta \right) \right] \cdot \boldsymbol{Z}^c \cdot \left[\boldsymbol{g}^\circ - \tfrac{1}{h^c} \left(2 \boldsymbol{v}^\Delta + (h^c + h^\circ) \boldsymbol{\varphi}^\circ + h^\Delta \boldsymbol{\varphi}^\Delta \right) \right] \\
& + \delta \boldsymbol{K}^\circ : \mathbb{D}^\circ : \boldsymbol{K}^\circ + \delta \boldsymbol{K}^\Delta : \mathbb{D}^\circ : \boldsymbol{K}^\Delta + \delta \boldsymbol{K}^\circ : \mathbb{D}^\Delta : \boldsymbol{K}^\Delta + \delta \boldsymbol{K}^\Delta : \mathbb{D}^\Delta : \boldsymbol{K}^\circ \\
& + \frac{1}{(h^c)^2} \left[2\delta \boldsymbol{G}^\Delta + h^\circ \delta \boldsymbol{K}^\circ + h^\Delta \delta \boldsymbol{K}^\Delta \right] : \mathbb{D}^c : \left[2 \boldsymbol{G}^\Delta + h^\circ \boldsymbol{K}^\circ + h^\Delta \boldsymbol{K}^\Delta \right] \Big\} \, d\Re,
\end{aligned}
\tag{35a}
$$

and the virtual external work

$$
\begin{aligned}
\delta W_{\text{ext}} = \int_{\partial \Re_p} \Big\{ & \left[\delta \boldsymbol{v}^\circ + \tfrac{1}{2} h^\Delta \delta \boldsymbol{\varphi}^\circ \right] \cdot \boldsymbol{n}_\nu^\circ + \left[\delta \boldsymbol{v}^\Delta + \tfrac{1}{2} (h^c + h^\circ) \delta \boldsymbol{\varphi}^\circ \right] \cdot \boldsymbol{n}_\nu^\Delta \\
& + \tfrac{1}{2} h^\circ \delta \boldsymbol{\varphi}^\Delta \cdot \boldsymbol{n}_\nu^c + \delta w q_\nu^\circ + \delta \boldsymbol{\varphi}^\circ \cdot \boldsymbol{m}_\nu^\circ + \delta \boldsymbol{\varphi}^\Delta \cdot \boldsymbol{m}_\nu^\Delta \\
& - \tfrac{1}{h^c} \left[2\delta \boldsymbol{v}^\Delta + (h^c + h^\circ) \delta \boldsymbol{\varphi}^\circ + h^\Delta \delta \boldsymbol{\varphi}^\Delta \right] \cdot \boldsymbol{m}_\nu^c \Big\} \, d\partial \Re_p \\
& + \int_{\Re_p} \left[\frac{h^t}{2} \left(\delta \boldsymbol{\varphi}^\circ + \delta \boldsymbol{\varphi}^\Delta \right) \cdot \boldsymbol{s} - \left(\delta \boldsymbol{v}^\circ + \delta \boldsymbol{v}^\Delta \right) \cdot \boldsymbol{s} + \delta w p \right] d\Re_p
\end{aligned}
\tag{35b}
$$

Hereby, $\Re_p$ and $\partial \Re_p$ denote the area and boundary of the reference surface $\Re$, where boundary conditions with respect to the stress resultants are prescribed.

$$
\left.
\begin{aligned}
\boldsymbol{N}_p^K &= \boldsymbol{N}^K \big|_{\partial \Re_p} \\
\boldsymbol{L}_p^K &= \boldsymbol{L}^K \big|_{\partial \Re_p} \\
\boldsymbol{q}_p^K &= \boldsymbol{q}^K \big|_{\partial \Re_p}
\end{aligned}
\right\} \; \forall \; K \in \{\circ, \Delta, c\}
\tag{36}
$$

Furthermore, stress resultants on the boundary of the surface continuum have been introduced.

$$
\left.
\begin{aligned}
\boldsymbol{n}_\nu^K &= \boldsymbol{v} \cdot \boldsymbol{N}_p^K \\
\boldsymbol{m}_\nu^K &= \boldsymbol{v} \cdot \boldsymbol{L}_p^K \\
q_\nu^K &= \boldsymbol{v} \cdot \boldsymbol{q}_p^K
\end{aligned}
\right\} \; \forall \; K \in \{\circ, \Delta, c\}
\tag{37}
$$

However, we can identify nine independent global degrees of freedom, i.e. v_1°, v_2°, v_1^Δ, v_2^Δ, w, φ_1°, φ_2°, φ_1^Δ, and φ_2^Δ.

2.2 Computational Implementation

The FEM is based on a strict separation of structural Ω and element level Ω^e.

$$
\Omega = \bigcup_{e=1}^{NE} \Omega^e \qquad\qquad \Omega^i \cap \Omega^j = \emptyset \quad \text{for } i \neq j \quad \text{while } i, j = \{1 \ldots NE\}
\tag{38}
$$

In what follows we utilize quadrilateral elements of Ω^e. However, the virtual works of the overall domain are formed by the summation of the individual contributions of the sub-domains, i.e. of the finite elements.

$$
\delta W_{\text{int}} = \sum_{e=1}^{NE} \delta W_{\text{int}}^e \qquad\qquad \delta W_{\text{ext}} = \sum_{e=1}^{NE} \delta W_{\text{ext}}^e
\tag{39}
$$

Herein, NE is the number of elements in the overall domain. In the sequel, for reasons of practicability, we make use of the vector-matrix notation, cf. Voigt (1889). In principle, the present approach is in accordance with the procedure presented in Eisenträger et al. (2015) while we here give a detailed disclosure of the computational implementation. However, the origin for the numerical implementation certainly lies in the work of Simo and Fox (1989) and Simo et al. (1989).

2.2.1 Approximation of Field Quantities

In present context it is sufficient to use the two-dimensional position vector for the geometrical description of a material point at the reference surface $\mathfrak{R}$.

$$\mathbf{x} = \begin{bmatrix} X_1 & X_2 \end{bmatrix}^\top \tag{40}$$

This is possible since we have reduced our concern to a global coordinate system $\{e_\alpha, \boldsymbol{n}\}$ with the definition of a reference surface $\mathfrak{R}$ which coincides with the mid surface of the core layer. Thus all layers can be represented by only one element in thickness direction. In order to discretize equations, the vector of DOF's at every node i is specified as follows.

$$\mathbf{a}^i = \begin{bmatrix} v_1^{\circ i} & v_2^{\circ i} & v_1^{\Delta i} & v_2^{\Delta i} & w^i & \varphi_1^{\circ i} & \varphi_2^{\circ i} & \varphi_1^{\Delta i} & \varphi_2^{\Delta i} \end{bmatrix}^\top \qquad \forall\, i = \{1, \dots, NN\} \tag{41}$$

while $NN = 8$ is the number of nodes per element for the present implementation. It becomes apparent that this definition results from the introduction of global degrees of freedom as presented in Eqs. (29a) and (29b). All node vectors of the degrees of freedom are combined in the element vector.

$$\mathbf{a}^e = \begin{bmatrix} \mathbf{a}^1 & \mathbf{a}^2 & \mathbf{a}^3 & \dots & \mathbf{a}^{NN} \end{bmatrix}^\top \tag{42}$$

In order to obtain the fields of DOF's over the element with respect to the natural coordinates $\boldsymbol{\xi}$, the DOF's are interpolated into the shape functions, applying the isoparametric element concept.

$$\mathbf{a}(\boldsymbol{\xi}) = \begin{bmatrix} v_1^\circ(\boldsymbol{\xi}) & v_2^\circ(\boldsymbol{\xi}) & v_1^\Delta(\boldsymbol{\xi}) & v_2^\Delta(\boldsymbol{\xi}) & w(\boldsymbol{\xi}) & \varphi_1^\circ(\boldsymbol{\xi}) & \varphi_2^\circ(\boldsymbol{\xi}) & \varphi_1^\Delta(\boldsymbol{\xi}) & \varphi_2^\Delta(\boldsymbol{\xi}) \end{bmatrix}^\top \approx \mathbf{N}(\boldsymbol{\xi})\, \mathbf{a}^e \tag{43}$$

Herein $\mathbf{N}(\boldsymbol{\xi})$ is the matrix of shape functions.

$$\mathbf{N}(\boldsymbol{\xi}) = \begin{bmatrix} \mathbf{N}^1(\boldsymbol{\xi}) & \mathbf{N}^2(\boldsymbol{\xi}) & \dots & \mathbf{N}^{NN}(\boldsymbol{\xi}) \end{bmatrix} \tag{44}$$

2.2.2 Shape Functions and Coordinate Transformations

As demonstrated, shape functions have to be introduced to approximate solutions. In the sequel we make use of SERENDIPITY-type shape functions, i.e. introduce functions of the polynomial degree $PG = 2$ (Szabó and Babuška, 1991).

$$N^i(\boldsymbol{\xi}) = {}^1\!/\!4 \left[1 + \xi_1^i \xi_1 \right] \left[1 + \xi_2^i \xi_2 \right] \left[\xi_1^i \xi_1 + \xi_2^i \xi_2 - 1 \right] \qquad i \in \{1, \dots, 4\} \tag{45a}$$

$$N^i(\boldsymbol{\xi}) = {}^1\!/\!2 \left[1 + \xi_1^i \xi_1 \right] \left[1 - \xi_2^2 \right] \qquad\qquad i \in \{6, 8\} \tag{45b}$$

$$N^i(\boldsymbol{\xi}) = {}^1\!/\!2 \left[1 + \xi_2^i \xi_2 \right] \left[1 - \xi_1^2 \right] \qquad\qquad i \in \{5, 7\} \tag{45c}$$

With the aid of these shape functions, we can assemble the matrix of shape functions at every node i.

$$\mathbf{N}^i(\boldsymbol{\xi}) = N^i(\boldsymbol{\xi})\,\mathbf{I}, \tag{46}$$

Thereby, $\mathbf{I}$ is a unit matrix, whose number of columns and rows is equal to the number of DOF's per node. This interpolation is performed in the natural coordinates of the finite element $-1 \le \xi_\alpha \le 1 \ \forall\, \alpha \in \{1, 2\}$. Since the functions are represented by isoparametric coordinates, a transformation relation between the two coordinate systems (physical and natural) is sought. This is realized via the so called Jacobi matrix $\mathbf{J}(\boldsymbol{\xi})$. In two dimensions, the transformations can be represented as follows (Oñate, 2013).

$$\frac{\partial}{\partial \boldsymbol{\xi}} = \mathbf{J}(\boldsymbol{\xi})\, \frac{\partial}{\partial \mathbf{x}} \qquad\qquad \frac{\partial}{\partial \mathbf{x}} = \mathbf{J}(\boldsymbol{\xi})^{-1}\, \frac{\partial}{\partial \boldsymbol{\xi}} \tag{47}$$

The Jacobi matrices and the individual derivatives are as follows.

$$\mathbf{J}(\boldsymbol{\xi}) = \begin{bmatrix} \dfrac{\partial X_1}{\partial \xi_1} & \dfrac{\partial X_2}{\partial \xi_1} \\[2ex] \dfrac{\partial X_1}{\partial \xi_2} & \dfrac{\partial X_2}{\partial \xi_2} \end{bmatrix} \qquad\qquad \mathbf{J}(\boldsymbol{\xi})^{-1} = \frac{1}{|\mathbf{J}(\boldsymbol{\xi})|} \begin{bmatrix} \dfrac{\partial X_2}{\partial \xi_2} & -\dfrac{\partial X_2}{\partial \xi_1} \\[2ex] -\dfrac{\partial X_1}{\partial \xi_2} & \dfrac{\partial X_1}{\partial \xi_1} \end{bmatrix} \tag{48}$$

2.2.3 Kinematic Relations

We hereby introduce global deformation measures $\mathbf{e}$ for the membrane (index M), bending (index B), and the transverse shear state (index S).

$$\mathbf{e}_{\text{MB}}(\boldsymbol{\xi}) = \begin{bmatrix} \mathbf{e}_M^\circ & \mathbf{e}_M^\Delta & \mathbf{e}_B^\circ & \mathbf{e}_B^\Delta \end{bmatrix}^\top \qquad\qquad \mathbf{e}_S(\boldsymbol{\xi}) = \begin{bmatrix} \mathbf{e}_S^\circ & \mathbf{e}_S^\Delta \end{bmatrix}^\top \tag{49}$$

The sub measures introduced therein are defined as follows.

$$\mathbf{e}_M^\circ = \begin{bmatrix} G_{11}^\circ & G_{22}^\circ & 2G_{12}^\circ \end{bmatrix}^\top = \begin{bmatrix} v_{1,1}^\circ & v_{2,2}^\circ & v_{1,2}^\circ + v_{2,1}^\circ \end{bmatrix}^\top \tag{50a}$$

$$\mathbf{e}_M^\vartriangle = \begin{bmatrix} G_{11}^\vartriangle & G_{22}^\vartriangle & 2G_{12}^\vartriangle \end{bmatrix}^\top = \begin{bmatrix} v_{1,1}^\vartriangle & v_{2,2}^\vartriangle & v_{1,2}^\vartriangle + v_{2,1}^\vartriangle \end{bmatrix}^\top \tag{50b}$$

$$\mathbf{e}_B^\circ = \begin{bmatrix} K_{11}^\circ & K_{22}^\circ & 2K_{12}^\circ \end{bmatrix}^\top = \begin{bmatrix} \varphi_{1,1}^\circ & \varphi_{2,2}^\circ & \varphi_{1,2}^\circ + \varphi_{2,1}^\circ \end{bmatrix}^\top \tag{50c}$$

$$\mathbf{e}_B^\vartriangle = \begin{bmatrix} K_{11}^\vartriangle & K_{22}^\vartriangle & 2K_{12}^\vartriangle \end{bmatrix}^\top = \begin{bmatrix} \varphi_{1,1}^\vartriangle & \varphi_{2,2}^\vartriangle & \varphi_{1,2}^\vartriangle + \varphi_{2,1}^\vartriangle \end{bmatrix}^\top \tag{50d}$$

$$\mathbf{e}_S^\circ = \begin{bmatrix} g_1^\circ & g_2^\circ \end{bmatrix}^\top \qquad = \begin{bmatrix} w_{,1} + \varphi_1^\circ & w_{,2} + \varphi_2^\circ \end{bmatrix}^\top \tag{50e}$$

$$\mathbf{e}_S^\vartriangle = \begin{bmatrix} g_1^\vartriangle & g_2^\vartriangle \end{bmatrix}^\top \qquad = \begin{bmatrix} \varphi_1^\vartriangle & \varphi_2^\vartriangle \end{bmatrix}^\top \tag{50f}$$

All of aforementioned measures represent fields, i.e. they depend on the natural coordinates. However, for reasons of space this dependency was not explicitly specified here. These deformation fields are approximated analogously to the degrees of freedom.

$$\mathbf{e}_{MB}(\xi) \approx \mathbf{B}_{MB}(\xi)\,\mathbf{a}^e \qquad\qquad\qquad \mathbf{e}_S(\xi) \approx \mathbf{B}_S(\xi)\,\mathbf{a}^e \tag{51}$$

The $\mathbf{B}$ matrices are compiled from the differential operator $\mathbf{D}$ and the matrix of the shape functions $\mathbf{N}$.

$$\mathbf{B}_{MB}(\xi) = \mathbf{D}_{MB}\mathbf{N}(\xi) \qquad \mathbf{B}_S(\xi) = \mathbf{D}_S\mathbf{N}(\xi) \tag{52}$$

The construction of the matrices $\mathbf{B}$ and $\mathbf{D}$ is given in App. A.1.

2.2.4 Constitutive Equations

To implement the constitutive laws, the expressions of the virtual work must be converted into vector-matrix notation also. The basic procedure for transferring constitutive quantities is given in App. A.1. The constitutive equations of the composite level are as follows while we introduce $\mathbf{s}$ as global kinetic measure.

$$\mathbf{s}_M^\circ = \left(\hat{\mathbf{C}}_M^\circ + \hat{\mathbf{C}}_M^c\right)\mathbf{e}_M^\circ + \hat{\mathbf{C}}_M^\vartriangle\mathbf{e}_M^\vartriangle + \frac{1}{2}\hat{\mathbf{C}}_M^c\left(h^\vartriangle\mathbf{e}_B^\circ + h^\circ\mathbf{e}_B^\vartriangle\right) \tag{53a}$$

$$\mathbf{s}_M^\vartriangle = \hat{\mathbf{C}}_M^\circ\mathbf{e}_M^\vartriangle + \hat{\mathbf{C}}_M^\vartriangle\mathbf{e}_M^\circ \tag{53b}$$

$$\mathbf{s}_M^c = \hat{\mathbf{C}}_M^c\left[\mathbf{e}_M^\circ + \frac{1}{2}\left(h^\vartriangle\mathbf{e}_B^\circ + h^\circ\mathbf{e}_B^\vartriangle\right)\right] \tag{53c}$$

$$\mathbf{s}_S^\circ = \hat{\mathbf{C}}_S^\circ\mathbf{e}_S^\circ + \hat{\mathbf{C}}_S^\vartriangle\mathbf{e}_S^\vartriangle + \hat{\mathbf{C}}_S^c\left(\mathbf{e}_S^\circ + \mathbf{A}_1\mathbf{a}\right) \tag{53d}$$

$$\mathbf{s}_S^\vartriangle = \hat{\mathbf{C}}_S^\circ\mathbf{e}_S^\vartriangle + \hat{\mathbf{C}}_S^\vartriangle\mathbf{e}_S^\circ \tag{53e}$$

$$\mathbf{s}_S^c = \hat{\mathbf{C}}_S^c\left(\mathbf{e}_S^\circ + \mathbf{A}_1\mathbf{a}\right) \tag{53f}$$

$$\mathbf{s}_B^\circ = \hat{\mathbf{C}}_B^\circ\mathbf{e}_B^\circ + \hat{\mathbf{C}}_B^\vartriangle\mathbf{e}_B^\vartriangle - \frac{1}{h^c}\hat{\mathbf{C}}_B^c\left(2\mathbf{e}_M^\vartriangle + h^\circ\mathbf{e}_B^\circ + h^\vartriangle\mathbf{e}_B^\vartriangle\right) - \frac{1}{2}\hat{\mathbf{C}}_M^\circ\left[h^\vartriangle\mathbf{e}_M^\circ + (h^c + h^\circ)\,\mathbf{e}_M^\vartriangle\right] - \frac{1}{2}\hat{\mathbf{C}}_M^\vartriangle\left[h^\vartriangle\mathbf{e}_M^\vartriangle + (h^c + h^\circ)\,\mathbf{e}_M^\circ\right] \tag{53g}$$

$$\mathbf{s}_B^\vartriangle = \hat{\mathbf{C}}_B^\circ\mathbf{e}_B^\vartriangle + \hat{\mathbf{C}}_B^\vartriangle\mathbf{e}_B^\circ \tag{53h}$$

$$\mathbf{s}_B^c = -\frac{1}{h^c}\hat{\mathbf{C}}_B^c\left(2\mathbf{e}_M^\vartriangle + h^\circ\mathbf{e}_B^\circ + h^\vartriangle\mathbf{e}_B^\vartriangle\right) \tag{53i}$$

The constitutive matrices $\hat{\mathbf{C}}_M^K$, $\hat{\mathbf{C}}_B^K$, $\hat{\mathbf{C}}_S^K \ \forall K \in \{\circ, \vartriangle, c\}$ and the auxiliary matrix $\mathbf{A}_1$ introduced here are enclosed in App. A.1.

2.2.5 Spatial Discretization of Virtual Work

The virtual internal work from Eq. (35a) can now be rewritten as follows.

$$\delta W_{\text{int}}^e = \int\limits_{\Omega^e} \delta\mathbf{a}^{e\top}\Bigg[\mathbf{B}_S^\top\left(\mathbf{C}_S^\circ + \mathbf{C}_S^\vartriangle + \mathbf{C}_S^{\vartriangle\top} + \mathbf{A}_2^\top\hat{\mathbf{C}}_S^c\mathbf{A}_2\right)\mathbf{B}_S + \mathbf{B}_S^\top\mathbf{A}_2^\top\hat{\mathbf{C}}_S^c\mathbf{A}_1\mathbf{N} + \left(\mathbf{B}_S^\top\mathbf{A}_2^\top\hat{\mathbf{C}}_S^c\mathbf{A}_1\mathbf{N}\right)^\top + \mathbf{N}^\top\mathbf{A}_1^\top\hat{\mathbf{C}}_S^c\mathbf{A}_1\mathbf{N}$$

$$+ \mathbf{B}_{MB}^\top\left(\mathbf{C}_{MB}^\circ + \mathbf{C}_{MB}^\vartriangle + \mathbf{C}_{MB}^{\vartriangle\top} + \mathbf{A}_3^\top\hat{\mathbf{C}}_M^c\mathbf{A}_3 + \mathbf{A}_4^\top\hat{\mathbf{C}}_B^c\mathbf{A}_4\right)\mathbf{B}_{MB}\Bigg]\mathbf{a}^e\,\mathrm{d}\Omega^e \tag{54}$$

In addition to the material properties in $\mathbf{C}_\square^K$ und $\hat{\mathbf{C}}_\square^K \ \forall \square \in \{M, B, MB, S\} \wedge K \in \{\circ, \vartriangle, c\}$, the expression now only contains the degrees of freedom $[\mathbf{a}^e]^\top$. $\mathbf{A}_i \ \forall i \in \{2, 3, 4\}$ are auxiliary matrices so that all quantities correspond to the specified vector of degrees of freedom. The detailed structure of all matrices from (54) can be found in App. A.1. Now we can get the stiffness matrices for membrane-bending and transverse shear separately.

$$\mathbf{K}_{MB}^e = \int\limits_{\Omega^e}\left[\mathbf{B}_{MB}^\top\left(\mathbf{C}_{MB}^\circ + \mathbf{C}_{MB}^\vartriangle + \mathbf{C}_{MB}^{\vartriangle\top} + \mathbf{A}_3^\top\hat{\mathbf{C}}_M^c\mathbf{A}_3 + \mathbf{A}_4^\top\hat{\mathbf{C}}_B^c\mathbf{A}_4\right)\mathbf{B}_{MB}\right]\mathrm{d}\Omega^e \tag{55a}$$

$$\mathbf{K}_S^e = \int\limits_{\Omega^e}\left[\mathbf{B}_S^\top\left(\mathbf{C}_S^\circ + \mathbf{C}_S^\vartriangle + \mathbf{C}_S^{\vartriangle\top} + \mathbf{A}_2^\top\hat{\mathbf{C}}_S^c\mathbf{A}_2\right)\mathbf{B}_S + \mathbf{B}_S^\top\mathbf{A}_2^\top\hat{\mathbf{C}}_S^c\mathbf{A}_1\mathbf{N} + \left(\mathbf{B}_S^\top\mathbf{A}_2^\top\hat{\mathbf{C}}_S^c\mathbf{A}_1\mathbf{N}\right)^\top + \mathbf{N}^\top\mathbf{A}_1^\top\hat{\mathbf{C}}_S^c\mathbf{A}_1\mathbf{N}\right]\mathrm{d}\Omega^e \tag{55b}$$

The separation is introduced to counter artificial stiffening effects correlated to transverse shear locking. The overall stiffness matrix is now additively composed of both sub matrices.

$$\mathbf{K}^e = \mathbf{K}^e_{\mathrm{MB}} + \mathbf{K}^e_{\mathrm{S}} \tag{56}$$

Eq. (35b) is converted in an analogous way. This results in the following expression.

$$\delta W^e_{\mathrm{ext}} = \int_{\partial\Omega^e_{\mathrm{p}}} \delta\mathbf{a}^{e\top}\mathbf{N}^\top\mathbf{A}_5\mathbf{t}\,\mathrm{d}\,\partial\Omega^e_{\mathrm{p}} + \int_{\Omega^e} \delta\mathbf{a}^{e\top}\mathbf{N}^\top\mathbf{q}\,\mathrm{d}\Omega^e \tag{57}$$

The vectors $\mathbf{t}$ and $\mathbf{q}$ contain loads distributed over a curve or a surface.

$$\mathbf{t} = \begin{bmatrix} \mathbf{n}^\circ_\nu & \mathbf{n}^\Delta_\nu & \mathbf{n}^c_\nu & q^\circ_\nu & \mathbf{m}^\circ_\nu & \mathbf{m}^\Delta_\nu & \mathbf{m}^c_\nu \end{bmatrix}^\top \tag{58}$$

$$\mathbf{q} = \begin{bmatrix} -s_1 & -s_2 & -s_1 & -s_2 & p & \frac{h^t}{2}s_1 & \frac{h^t}{2}s_2 & \frac{h^t}{2}s_1 & \frac{h^t}{2}s_2 \end{bmatrix}^\top \tag{59}$$

The vectors $\mathbf{n}^\circ_\nu$, $\mathbf{n}^\Delta_\nu$, $\mathbf{n}^c_\nu$, $\mathbf{m}^\circ_\nu$, $\mathbf{m}^\Delta_\nu$, and $\mathbf{m}^c_\nu$ refer to expressions in Eq. (37), which are given there in tensor notation. These can be converted into vector-matrix notation and referenced to the domain element Ω^e. However, the right-hand-side vector $\mathbf{r}^e$ comprises line loads $\mathbf{r}^e_1$ and surface loads $\mathbf{r}^e_2$ on the element.

$$\mathbf{r}^e = \mathbf{r}^e_1 + \mathbf{r}^e_2 \tag{60}$$

The sub vectors are determined as follows.

$$\mathbf{r}^e_1 = \int_{\partial\Omega^e_{\mathrm{p}}} \mathbf{N}^\top\mathbf{A}_5\mathbf{t}\,\mathrm{d}\,\partial\Omega^e_{\mathrm{p}} \qquad\qquad \mathbf{r}^e_2 = \int_{\Omega^e_{\mathrm{p}}} \mathbf{N}^\top\mathbf{q}\,\mathrm{d}\Omega^e_{\mathrm{p}} \tag{61}$$

2.2.6   Assembly and Structural Equation

Structure level quantities are generated by summing all elements $e \in [1, NE]$ in Ω. In symbolic notation we make use of the $\cup$ operator.

$$\mathbf{K} = \bigcup_{e=1}^{NE}\mathbf{K}^e \qquad\qquad \mathbf{a} = \bigcup_{e=1}^{NE}\mathbf{a}^e \qquad\qquad \mathbf{r} = \bigcup_{e=1}^{NE}\mathbf{r}^e \tag{62}$$

Though this assembling we can formulate the spatially approximated weak form.

$$\begin{aligned} \delta W_{\mathrm{int}} &= \delta W_{\mathrm{ext}} \\ \delta\mathbf{a}\cdot\mathbf{K}\,\mathbf{a} &= \delta\mathbf{a}\cdot\mathbf{r} \end{aligned} \tag{63}$$

From Eqs. (34) and (39) it can be deduced that the sum of the virtual works must be zero.

$$\delta W \approx \delta\mathbf{a}\cdot[\mathbf{K}\,\mathbf{a} - \mathbf{r}] = 0 \tag{64}$$

For arbitrary virtual degrees of freedom $\delta\mathbf{a}$ the discrete equation of motion is obtained.

$$\mathbf{K}\,\mathbf{a} = \mathbf{r} \tag{65}$$

The solution of this system of equations is realized by the left-hand multiplication with the inverse of the stiffness matrix $\mathbf{K}^{-1}$.

$$\mathbf{K}^{-1}\mathbf{K}\,\mathbf{a} = \mathbf{I}\,\mathbf{a} = \mathbf{a} = \mathbf{K}^{-1}\,\mathbf{r} \tag{66}$$

The stiffness matrix must not be singular, since the invertibility is then no longer guaranteed. In order to prevent this, so many Dirichlet boundary conditions must be introduced into the structural equation that no rigid body motions are possible. However, in present context we made use of the finite element program system ABAQUS. To solve problems in the manner set forth above, we have programmed a user-defined element (UEL) in a FORTRAN subroutine.

3   Application Range

3.1   Preliminary Remarks

In present contribution we want to emphasize the universality of the proposed approach by highlighting the range of applicability. To be more precise, we seek to determine the broadness in the filed of TLCS. Therefore, we will execute parameter studies at the simple case of constant, homogeneous, and orthogonal loading with a small test load while free supports are applied at all layer boundaries with normals $\boldsymbol{e}_\alpha$. The spatial discretization is realized via an structured mesh where all elements show an aspect ratio $AR = {}^{h^e_{\max}}\!/\!_{h^e_{\min}} = 1$ while all elements feature inner angles with 90°. Herein, h^e_α is the element edge length. The mesh grid is
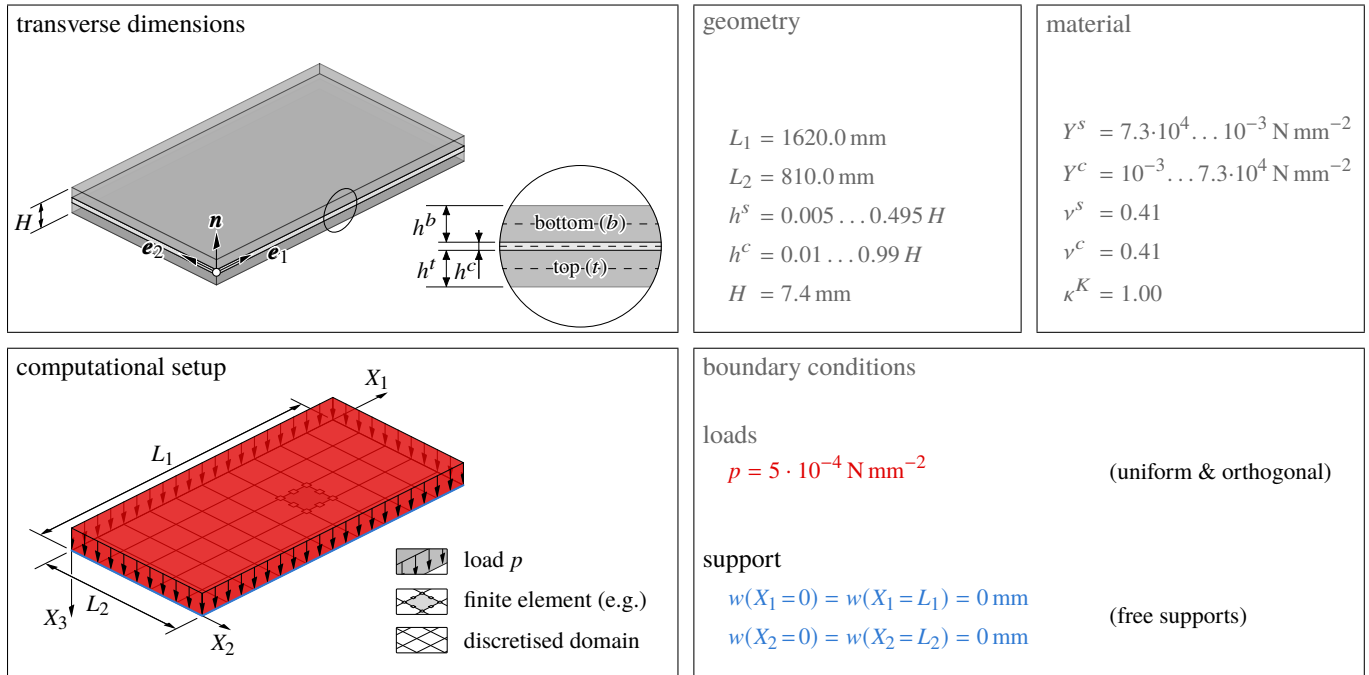
Fig. 4: Geometry, material, boundary conditions and discretization to determine the range of application of present approach

$256 \times 128 = 32768$ elements ($h_\alpha^e \approx 6.33$ mm) to guarantee convergence for all subsequent scrutinies. For the sake of simplicity we reduce our concern to a symmetric composite structure. Therefore, the following relations holds true, while we introduce the superscript index s for the skin layers.

$$h^t = h^b = h^s \qquad\qquad Y^t = Y^b = Y^s \qquad\qquad \nu^t = \nu^b = \nu^s \qquad\qquad (67)$$

Consequently, the following also applies.

$$B^t = B^b = B^s \qquad G^t = G^b = G^s \qquad D_\square^t = D_\square^b = D_\square^s \qquad \forall \square \in \{M, B, S\} \qquad (68)$$

We consider a test structure with plane dimensions $L_1 = 1620$ mm and $L_2 = 810$ mm as exemplary values. For present work we want to investigate the limit behavior for three-layered composite structures. Therefore, we introduce two geometrical limiting cases and a transversely evenly distributed geometrical case in context of aforementioned restrictions. These are as follows.

- $h^c = h^s$ (even distributed)
- $h^c = 0.99 H$ (thick core bound)
- $h^c = 0.01 H$ (thin core bound)

The corresponding skin layer thicknesses arise from the restriction for the overall thickness H.

$$h^s = \frac{H - h^c}{2} \qquad\qquad H \overset{!}{=} 7.4 \text{ mm} \qquad (69)$$

For the evenly distributed (equal thicknesses) composite this results in a transverse geometry with $h^k = {}^{37}/_{15}$ mm $\forall K \in \{c, s\}$. The thin core bound is characterized by $h^c = 0.074$ mm while the thick core is by $h^c = 7.326$ mm. However, for all cases it becomes obvious that $L_\alpha \gg H$ holds true.
To determine the working range of XLWT we vary the shear modulus ratio GR, which is a significant measure of the diverging material properties of core and skin layers, determined as follows.

$$GR = \frac{G^c}{G^s} \qquad (70)$$

For the sake of simplicity, we reduce our concern to transverse shear correction factors $\kappa^K \equiv 1 \ \forall K \in \{t, c, b\}$. The variety of material parameters is given Fig. 4. This results in a shear modulus ratio $GR_{\min}$ below 10^{-7} for present investigations, i.e. a maximum difference of more than seven magnitudes of order between the shear moduli alone. In present investigations, this also applies to the Young's modulus ratio $YR = {}^{Y^c}/_{Y^s}$ since $\nu^c = \nu^s$ holds. In this context, the designation *high contrast plates* retains validity. However, we reduce our concern to the case of $GR \leq 1$. In connection with engineering applications, this represents a reasonable limit. Applications with soft skins while the core is stiff seem extremely uncommon. For the opposite limit therefore $GR_{\max} = 1$ holds. Therewith, we can depict two bounds arising from monocoque structures known from theory. So it is possible to determine clearly, two, so-called monolithic limits. This is the shear-rigid monolith (Kirchhoff theory) and the shear-deformable monolith (Mindlin or Reissner theory). From these limits we carry out two investigations whereby we vary the shear modulus ratio through systematically. In a first attempt we decrease the shear modulus of the core layer G^c when starting
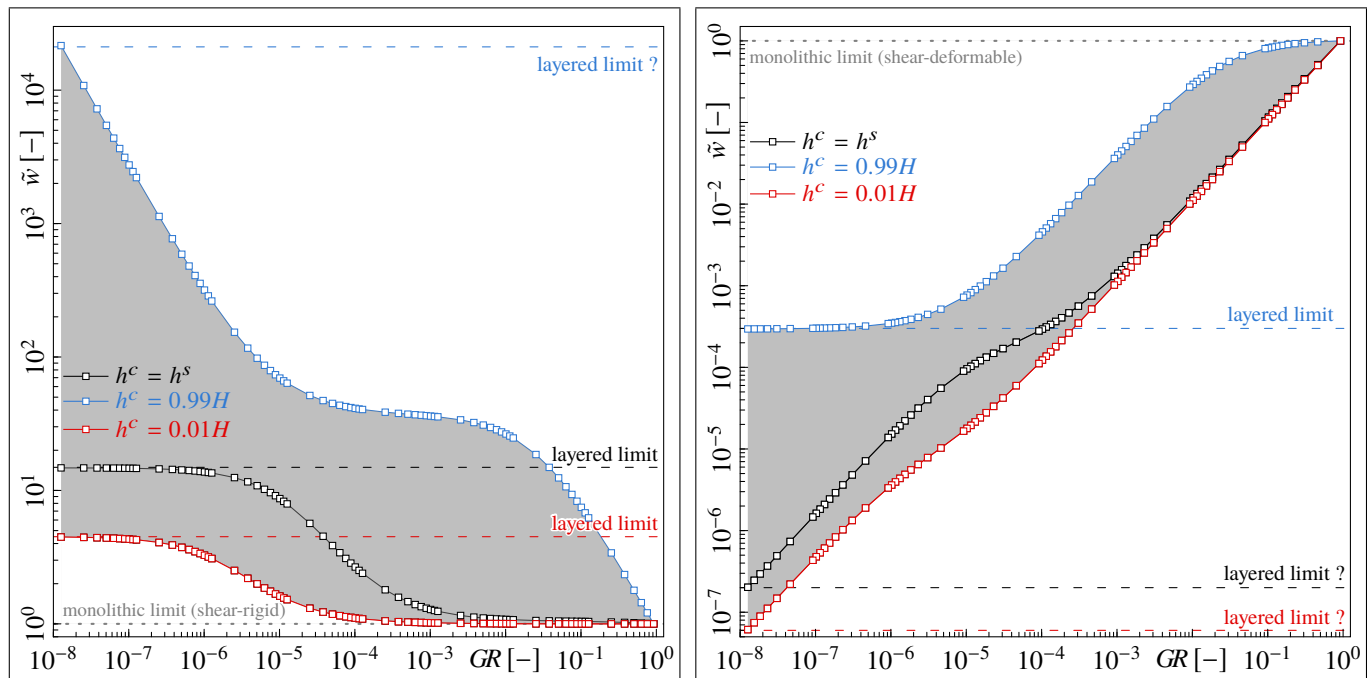
Fig. 5: Results of parameter studies starting from shear-rigid (left) and shear-deformable (right) monolithic limit of symmetric
TLCS

from $Y^c = Y^s = 73,000 \,^{N}/_{mm^2}$ ($\Rightarrow$ $GR = 1$, shear-rigid). The second attempt is implemented by the increase of the shear modulus of the skin layers G^s when starting from $Y^c = Y^s = 0.001 \,^{N}/_{mm^2}$ ($\Rightarrow$ $GR = 1$, but shear-deformable). As evaluation criterion we use the deflection of the composite. However, for all variations of GR, we normalize our results of the maximum deflection w_{max} in the following way for the admissible regime of GR.

$$\tilde{w} = \frac{w_{max}(GR)}{w_{max}(GR_{max})} \qquad\qquad w_{max} = w\left(^{x_\alpha}/_2\right) \qquad\qquad GR_{min} \leq GR \leq GR_{max} \qquad (71)$$

3.2 Results and Discussion

The results of present investigations are depicted in Fig. 5. On the left-hand side are the results of the examination starting from the shear-rigid monolithic limit and on the right-hand-side are the ones of the examination starting from the shear-deformable monolithic limit.

As previously indicated, for material and geometrical constellations we have used extremal parameters, at least in context of engineering applications (technical feasibility limits and limits of the sensuality). The range of application is localized by the thin core bound (lower bound) and the thick core bound (upper bound) for both procedures. Unsurprisingly, the even distributed composite lies between these two results. The course of the this even distributed composite follows that of the thin core bound. Also appears logical that deflections are increasing when starting present investigations from shear-rigid monolithic limit with decreasing G^c. Vice versa, deflections are decreasing when starting from shear-deformable monolithic limit while increasing G^s. For both investigations the range of application increases with decreasing shear modulus ratio. The results of all geometrical extremal cases coincide in the case $GR = 1$.

As can be found in some publications already (Naumenko and Eremeyev, 2014; Aßmus et al., 2017a), the thin core bound reaches its limits asymptotically when starting from a shear-rigid limit. This also applies to the even distributed composite. In both cases we can identify so called layered limits. This is the case when skin layers glide on each other with almost none resistance. However, for the thick core bound, such a limit does not exist when stating from a shear-rigid monolith. In addition, no asymptotic behavior can be detected either.

Contrary, when starting from the shear-deformable monolithic limit, the thick core bound exhibits an asymptotic behavior, while the layered limit of this bound is clearly identifiable. On the other hand, the existence of layered limits for both, thin core bound and even distributed composite are questionable, at least in the admissible range of GR.

In principle, it must therefore be stated that the use of the *eXtended layer-wise theory* presented here is indispensable, especially for cases in which no layered limit is achieved. However, it is precisely these limit cases that open up the scope of the approach presented here. By the best knowledge of the authors, there is no other known theory for the treatment of mechanical problems at three-layered composite structures with such a wide range of applicability. As already mentioned at the beginning, modern applications require such generalized approaches in order to meet the requirements of strongly diverging material pairings and geometry compositions.

For the sake of completeness, the numerical burden should be mentioned. The computation times were around 30 to 60 seconds on a standard pc (Intel i7-3820 processor, 32 GB RAM, 64 Bit Windows 7 operating system), depending on the material and geometrical constellations. Such short computation times emphasize the efficiency of the approach presented here.

M. Aßmus, K. Naumenko, A. Öchsner, V. A. Eremeyev, H. Altenbach

Tech. Mech., Vol. 39, Is. 2, (2019), 202–219

4 Concluding Remarks

4.1 Conclusion

In this work we have introduced a generalized framework for three-layered composite structures to consider strong divergent geometrical and material properties. This was done in the framework of a layer-wise procedure while starting by the aid of the direct approach. Therewith, present approach is geometrically exact. This expression arises from the exact kinematic representation of the two-dimensional surface. This means, that results gained are exact on the mid surface of the individual layer only. The restrictions introduced to couple layers are justifiable for engineering applications. There they will find a broad application, at least in the determination of composite stiffness relations.

In context of the computational solution procedure introduced, the approach to reduce all considerations to a single reference surface simplifies the calculation of present structures where at the same time a large number of composites with arbitrary properties can be computed. Furthermore, we only have low requirements on the shape functions and boundary conditions since present approach requires C^0 continuity only, i.e. only the DOFs themselves have to be continuous on the element boundaries (Hinton et al., 1990). That is a not negligible advantage over C^1 continuous elements as they are needed for the use of shear-rigid theories, i.e. when using the Kirchhoff theory (Kirchhoff, 1850).

We note that the purpose of this paper is to show the the broad scope of application and general valedness of the layer-wise model. In that sense, the first-order shear deformation theory and the classical laminate theory that are commonly used arise as special cases when different simplifications are imposed. This is surely also the case to what is known as sandwich theory which has not been identified in the context of present investigations. Some general examples for special cases at layer-level have been given in Aßmus et al. (2019), which show that plate model obtained by the direct approach attains universality, at least in context of engineering applications. However, the broadness of applicability of present layerwise generalisation seems unique.

4.2 Outlook

In present context we reduced our concern to the static load case, linear elastic material behaviour, and small deformations. As in classical continuum theory, extensions lie in the consideration of

- inertia,
- dynamic loading, and
- damping.

Regarding enlargements with respect to kinematics introduced, it is possible to consider

- moderate deformations, i.e.
  - large deflections
  - small in-plane displacements
  - small rotations
- or large deformations, i.e.
  - large deflections
  - large displacements
  - large rotations

while the latter being preferred in context of a consistent generalization. At least in this case, we also have to reformulate the kinematical restrictions (28a) and (28b). The constitutive relations can be extended to nonlinear elastic or inelastic behaviour, e.g.

- viscoelasticity,
- (visco-)plasticity,
- fatigue, and
- damage.

In addition, the consideration of anisotropic material behavior is certainly also a focal point. This may also have to include coupling effects between the different deformation states considered at layer-level, which until now have only been superimposed. All theses extensions hold true for the individual layers. However, within the modular structure of the approach presented here it is simple to enlarge its frame to analyze three-layered composite structures for arbitrary deformations, material behavior and loading conditions, at least up to the borders that exist in classical theory of three-dimensional continua (e.g. uniqueness, etc.). Couplings with thermodynamics, electrodynamics and other non-mechanical influences such as hygroscopic ones are also conceivable.

A special feature of the present approach using a layer-wise contemplation is the consideration of delamination. Thereby it is possible to relax the kinematical constraints (28a) and (28b) whereby advanced traction-separation laws for the interaction between the layers can be introduced.

However, present theory is based on whats known as plate or more generally shell theories. It is generally accepted, that such theories are not capable to prognosticate full and exact information concerning a three-dimensional body manifold which forms the basis of every treatment.

Acknowledgment

Appendix

A.1 Constitutive Relations in Vector-Matrix Formulation

Consequently, the matrices required in the FEM are to be given in terms of global variables (indices $\circ$, Δ, c) for the three layered composite in vector-matrix form. The constitutive tensors of the global quantities can be introduced in matrix notation as follows, introducing **C** as a global stiffness quantity for the sake of simplicity.

$$\hat{\mathbf{C}}_{\mathrm{M}}^{K} = \begin{bmatrix} a_{\mathrm{M}}^{K} + 2b_{\mathrm{M}}^{K} & b_{\mathrm{M}}^{K} & 0 \\ a_{\mathrm{M}}^{K} & a_{\mathrm{M}}^{K} + 2b_{\mathrm{M}}^{K} & 0 \\ 0 & 0 & b_{\mathrm{M}}^{K} \end{bmatrix} \qquad \forall\, K \in \{\circ, \Delta, c\} \tag{A.1a}$$

$$\hat{\mathbf{C}}_{\mathrm{B}}^{K} = \begin{bmatrix} a_{\mathrm{B}}^{K} + 2b_{\mathrm{B}}^{K} & b_{\mathrm{B}}^{K} & 0 \\ a_{\mathrm{B}}^{K} & a_{\mathrm{B}}^{K} + 2b_{\mathrm{B}}^{K} & 0 \\ 0 & 0 & b_{\mathrm{B}}^{K} \end{bmatrix} \qquad \forall\, K \in \{\circ, \Delta, c\} \tag{A.1b}$$

$$\hat{\mathbf{C}}_{\mathrm{S}}^{K} = a_{\mathrm{S}}^{K} \begin{bmatrix} 1 & 0 \\ 0 & 1 \end{bmatrix} \qquad \forall\, K \in \{\circ, \Delta, c\} \tag{A.1c}$$

Here, the following abbreviations have been introduced based on the engineering interpretations for membrane stiffness D_{M}, bending stiffness D_{B}, and transverse shear stiffness D_{S}.

$$a_{L}^{K} = \begin{cases} D_{L}^{t} v^{t} + D_{L}^{b} v^{b} & \text{if } K = \circ \\ D_{L}^{t} v^{t} - D_{L}^{b} v^{b} & \text{if } K = \Delta \\ D_{L}^{c} v^{c} & \text{if } K = c \end{cases} \qquad \forall\, L \in \{\mathrm{M}, \mathrm{B}\} \tag{A.2a}$$

$$b_{L}^{K} = \begin{cases} \frac{1-v^{t}}{2} D_{L}^{t} + \frac{1-v^{t}}{2} D_{L}^{b} & \text{if } K = \circ \\ \frac{1-v^{t}}{2} D_{L}^{t} - \frac{1-v^{t}}{2} D_{L}^{b} & \text{if } K = \Delta \\ \frac{1-v^{t}}{2} D_{L}^{c} & \text{if } K = c \end{cases} \qquad \forall\, L \in \{\mathrm{M}, \mathrm{B}\} \tag{A.2b}$$

$$a_{\mathrm{S}}^{K} = \begin{cases} D_{\mathrm{S}}^{t} + D_{\mathrm{S}}^{b} & \text{if } K = \circ \\ D_{\mathrm{S}}^{t} - D_{\mathrm{S}}^{b} & \text{if } K = \Delta \\ D_{\mathrm{S}}^{c} & \text{if } K = c \end{cases} \tag{A.2c}$$

With the above representation, the generalized stiffness matrices can be specified.

$$\mathbf{C}_{\mathrm{MB}}^{\circ} = \begin{bmatrix} \hat{\mathbf{C}}_{\mathrm{M}}^{\circ} & \mathbf{0} & \mathbf{0} & \mathbf{0} \\ \mathbf{0} & \hat{\mathbf{C}}_{\mathrm{M}}^{\circ} & \mathbf{0} & \mathbf{0} \\ \mathbf{0} & \mathbf{0} & \hat{\mathbf{C}}_{\mathrm{B}}^{\circ} & \mathbf{0} \\ \mathbf{0} & \mathbf{0} & \mathbf{0} & \hat{\mathbf{C}}_{\mathrm{B}}^{\circ} \end{bmatrix} \tag{A.3a}$$

$$\mathbf{C}_{\mathrm{MB}}^{\Delta} = \begin{bmatrix} \mathbf{0} & \hat{\mathbf{C}}_{\mathrm{M}}^{\Delta} & \mathbf{0} & \mathbf{0} \\ \mathbf{0} & \mathbf{0} & \mathbf{0} & \mathbf{0} \\ \mathbf{0} & \mathbf{0} & \mathbf{0} & \hat{\mathbf{C}}_{\mathrm{B}}^{\Delta} \\ \mathbf{0} & \mathbf{0} & \mathbf{0} & \mathbf{0} \end{bmatrix} \tag{A.3b}$$

$$\mathbf{C}_{\mathrm{S}}^{\circ} = \begin{bmatrix} \hat{\mathbf{C}}_{\mathrm{S}}^{\circ} & \mathbf{0} \\ \mathbf{0} & \hat{\mathbf{C}}_{\mathrm{S}}^{\circ} \end{bmatrix} \tag{A.3c}$$

$$\mathbf{C}_{\mathrm{S}}^{\Delta} = \begin{bmatrix} \mathbf{0} & \hat{\mathbf{C}}_{\mathrm{S}}^{\Delta} \\ \mathbf{0} & \mathbf{0} \end{bmatrix} \tag{A.3d}$$

The zero matrices in the Eq. (A.3a) and (A.3b) each possess three columns and rows, while the null matrices in Eq. (A.3c) und (A.3d) have only two columns and rows each. The **B** matrices for combining the approximation of local continuous kinematic measures with the discrete degrees of freedom of the element are given as follows.

$$\mathbf{B}_{\mathrm{MB}} = \begin{bmatrix} \mathbf{B}_{\mathrm{MB}_1} & \mathbf{B}_{\mathrm{MB}_2} & \cdots & \mathbf{B}_{\mathrm{MB}_{\mathscr{N}}} \end{bmatrix} \qquad\qquad \mathbf{B}_{\mathrm{MB}_i} = \begin{bmatrix} \hat{\mathbf{B}}_{\mathrm{M}_i}^{\circ} & \hat{\mathbf{B}}_{\mathrm{M}_i}^{\Delta} & \hat{\mathbf{B}}_{\mathrm{B}_i}^{\circ} & \hat{\mathbf{B}}_{\mathrm{B}_i}^{\Delta} \end{bmatrix}^{\top} \tag{A.4a}$$

$$\mathbf{B}_{\mathrm{S}} = \begin{bmatrix} \mathbf{B}_{\mathrm{S}_1} & \mathbf{B}_{\mathrm{S}_2} & \cdots & \mathbf{B}_{\mathrm{S}_{\mathscr{N}}} \end{bmatrix} \qquad\qquad \mathbf{B}_{\mathrm{S}_i} = \begin{bmatrix} \hat{\mathbf{B}}_{\mathrm{S}_i}^{\circ} & \hat{\mathbf{B}}_{\mathrm{S}_i}^{\Delta} \end{bmatrix}^{\top} \tag{A.4b}$$

The sub measures introduced herein are given in the following matrices.

$$
\hat{\mathbf{B}}^{\circ}_{\mathrm{M}_i} = \begin{bmatrix} N^i_{,1} & 0 & 0 & 0 & 0 & 0 & 0 & 0 & 0 \\ 0 & N^i_{,2} & 0 & 0 & 0 & 0 & 0 & 0 & 0 \\ N^i_{,2} & N^i_{,1} & 0 & 0 & 0 & 0 & 0 & 0 & 0 \end{bmatrix}
\tag{A.5a}
$$

$$
\hat{\mathbf{B}}^{\Delta}_{\mathrm{M}_i} = \begin{bmatrix} 0 & 0 & N^i_{,1} & 0 & 0 & 0 & 0 & 0 & 0 \\ 0 & 0 & 0 & N^i_{,2} & 0 & 0 & 0 & 0 & 0 \\ 0 & 0 & N^i_{,2} & N^i_{,1} & 0 & 0 & 0 & 0 & 0 \end{bmatrix}
\tag{A.5b}
$$

$$
\hat{\mathbf{B}}^{\circ}_{\mathrm{B}_i} = \begin{bmatrix} 0 & 0 & 0 & 0 & 0 & 0 & N^i_{,1} & 0 & 0 \\ 0 & 0 & 0 & 0 & 0 & -N^i_{,2} & 0 & 0 & 0 \\ 0 & 0 & 0 & 0 & 0 & -N^i_{,1} & N^i_{,2} & 0 & 0 \end{bmatrix}
\tag{A.5c}
$$

$$
\hat{\mathbf{B}}^{\Delta}_{\mathrm{B}_i} = \begin{bmatrix} 0 & 0 & 0 & 0 & 0 & 0 & 0 & 0 & N^i_{,1} \\ 0 & 0 & 0 & 0 & 0 & 0 & 0 & -N^i_{,2} & 0 \\ 0 & 0 & 0 & 0 & 0 & 0 & 0 & -N^i_{,1} & N^i_{,2} \end{bmatrix}
\tag{A.5d}
$$

$$
\hat{\mathbf{B}}^{\circ}_{\mathrm{S}_i} = \begin{bmatrix} 0 & 0 & 0 & 0 & N^i_{,1} & 0 & N^i & 0 & 0 \\ 0 & 0 & 0 & 0 & N^i_{,2} & -N^i & 0 & 0 & 0 \end{bmatrix}
\tag{A.5e}
$$

$$
\hat{\mathbf{B}}^{\Delta}_{\mathrm{S}_i} = \begin{bmatrix} 0 & 0 & 0 & 0 & 0 & 0 & 0 & 0 & N^i \\ 0 & 0 & 0 & 0 & 0 & 0 & 0 & -N^i & 0 \end{bmatrix}
\tag{A.5f}
$$

The differential operators for membrane, bending, and transverse shear state as well as their auxiliary matrices are structured as follows.

$$
\mathbf{D}_{\mathrm{MB}} = \begin{bmatrix} \mathbf{D}^{\circ}_{\mathrm{M}} & \mathbf{D}^{\Delta}_{\mathrm{M}} & \mathbf{D}^{\circ}_{\mathrm{B}} & \mathbf{D}^{\Delta}_{\mathrm{B}} \end{bmatrix}^{\top}
\tag{A.6a}
$$

$$
\mathbf{D}_{\mathrm{S}} = \begin{bmatrix} \mathbf{D}^{\circ}_{\mathrm{S}} & \mathbf{D}^{\Delta}_{\mathrm{S}} \end{bmatrix}^{\top}
\tag{A.6b}
$$

The sub operators used therein are structured as follows.

$$
\mathbf{D}^{\circ}_{\mathrm{M}} = \begin{bmatrix} \frac{\partial}{\partial X_1} & 0 & 0 & 0 & 0 & 0 & 0 & 0 & 0 \\ 0 & \frac{\partial}{\partial X_2} & 0 & 0 & 0 & 0 & 0 & 0 & 0 \\ \frac{\partial}{\partial X_2} & \frac{\partial}{\partial X_1} & 0 & 0 & 0 & 0 & 0 & 0 & 0 \end{bmatrix}
\tag{A.7a}
$$

$$
\mathbf{D}^{\Delta}_{\mathrm{M}} = \begin{bmatrix} 0 & 0 & \frac{\partial}{\partial X_1} & 0 & 0 & 0 & 0 & 0 & 0 \\ 0 & 0 & 0 & \frac{\partial}{\partial X_2} & 0 & 0 & 0 & 0 & 0 \\ 0 & 0 & \frac{\partial}{\partial X_2} & \frac{\partial}{\partial X_1} & 0 & 0 & 0 & 0 & 0 \end{bmatrix}
\tag{A.7b}
$$

$$
\mathbf{D}^{\circ}_{\mathrm{B}} = \begin{bmatrix} 0 & 0 & 0 & 0 & 0 & \frac{\partial}{\partial X_1} & 0 & 0 & 0 \\ 0 & 0 & 0 & 0 & 0 & 0 & \frac{\partial}{\partial X_2} & 0 & 0 \\ 0 & 0 & 0 & 0 & 0 & \frac{\partial}{\partial X_2} & \frac{\partial}{\partial X_1} & 0 & 0 \end{bmatrix}
\tag{A.7c}
$$

$$
\mathbf{D}^{\Delta}_{\mathrm{B}} = \begin{bmatrix} 0 & 0 & 0 & 0 & 0 & 0 & 0 & \frac{\partial}{\partial X_1} & 0 \\ 0 & 0 & 0 & 0 & 0 & 0 & 0 & 0 & \frac{\partial}{\partial X_2} \\ 0 & 0 & 0 & 0 & 0 & 0 & 0 & \frac{\partial}{\partial X_2} & \frac{\partial}{\partial X_1} \end{bmatrix}
\tag{A.7d}
$$

$$
\mathbf{D}^{\circ}_{\mathrm{S}} = \begin{bmatrix} 0 & 0 & 0 & 0 & \frac{\partial}{\partial X_1} & 1 & 0 & 0 & 0 \\ 0 & 0 & 0 & 0 & \frac{\partial}{\partial X_2} & 0 & 1 & 0 & 0 \end{bmatrix}
\tag{A.7e}
$$

$$
\mathbf{D}^{\Delta}_{\mathrm{S}} = \begin{bmatrix} 0 & 0 & 0 & 0 & 0 & 0 & 0 & 1 & 0 \\ 0 & 0 & 0 & 0 & 0 & 0 & 0 & 0 & 1 \end{bmatrix}
\tag{A.7f}
$$

The auxiliary matrices $\mathbf{A}_i \ \forall \ i \in \{1,\ldots,5\}$ for transforming the terms of virtual work into the vector-matrix notation are defined as follows.

$$\mathbf{A}_1 = \frac{1}{h^c} \begin{bmatrix} 0 & 0 & -2 & 0 & 0 & -(h^\circ + h^c) & 0 & -h^\Delta & 0 \\ 0 & 0 & 0 & -2 & 0 & 0 & -(h^\circ + h^c) & 0 & -h^\Delta \end{bmatrix} \tag{A.8a}$$

$$\mathbf{A}_2 = \begin{bmatrix} 1 & 0 & 0 & 0 \\ 0 & 1 & 0 & 0 \end{bmatrix} \tag{A.8b}$$

$$\mathbf{A}_3 = \begin{bmatrix} \mathbf{I} & \mathbf{0} & \frac{1}{2}h^\Delta\mathbf{I} & \frac{1}{2}h^\circ\mathbf{I} \end{bmatrix} \tag{A.8c}$$

$$\mathbf{A}_4 = \frac{1}{h^c} \begin{bmatrix} \mathbf{0} & 2\mathbf{I} & h^\circ\mathbf{I} & h^\Delta\mathbf{I} \end{bmatrix} \tag{A.8d}$$

$$\mathbf{A}_5 = \begin{bmatrix} 1 & 0 & 0 & 0 & 0 & 0 & 0 & 0 & 0 & 0 & 0 & 0 & 0 \\ 0 & 1 & 0 & 0 & 0 & 0 & 0 & 0 & 0 & 0 & 0 & 0 & 0 \\ 0 & 0 & 1 & 0 & 0 & 0 & 0 & 0 & 0 & 0 & 0 & -\frac{2}{h^c} & 0 \\ 0 & 0 & 0 & 1 & 0 & 0 & 0 & 0 & 0 & 0 & 0 & 0 & -\frac{2}{h^c} \\ 0 & 0 & 0 & 0 & 0 & 0 & 1 & 0 & 0 & 0 & 0 & 0 & 0 \\ \frac{1}{2}h^\Delta & 0 & \frac{1}{2}(h^\circ+h^c) & 0 & 0 & 0 & 0 & -1 & 0 & 0 & -\frac{h^\circ+h^c}{h^c} & 0 \\ 0 & \frac{1}{2}h^\Delta & 0 & \frac{1}{2}(h^\circ+h^c) & 0 & 0 & 0 & 1 & 0 & 0 & 0 & 0 & -\frac{h^\circ+h^c}{h^c} \\ 0 & 0 & 0 & 0 & \frac{1}{2}h^\circ & 0 & 0 & 0 & 0 & -1 & -\frac{h^\Delta}{h^c} & 0 \\ 0 & 0 & 0 & 0 & 0 & \frac{1}{2}h^\circ & 0 & 0 & 0 & 1 & 0 & 0 & -\frac{h^\Delta}{h^c} \end{bmatrix} \tag{A.8e}$$

The unit matrix $\mathbf{I}$ and the zero matrices $\mathbf{0}$ in Eqs. (A.8c)–(A.8d) feature three columns and rows each.

References

H. Altenbach and V. Eremeyev. Thin-walled structural elements: Classification, classical and advanced theories, new applications. In H. Altenbach and V. Eremeyev, editors, *Shell-like Structures: Advanced Theories and Applications*, pages 1–62. 2017. doi: 10.1007/978-3-319-42277-0_1.

M. Aßmus. *Structural Mechanics of Anti-Sandwiches. An Introduction*. SpringerBriefs in Continuum Mechanics. Springer, Cham, 2019. doi: 10.1007/978-3-030-04354-4.

M. Aßmus, S. Bergmann, K. Naumenko, and H. Altenbach. Mechanical behaviour of photovoltaic composite structures: A parameter study on the influence of geometric dimensions and material properties under static loading. *Composites Communications*, 5(-):23–26, 2017a. doi: 10.1016/j.coco.2017.06.003.

M. Aßmus, J. Eisenträger, and H. Altenbach. Projector representation of isotropic linear elastic material laws for directed surfaces. *Zeitschrift für Angewandte Mathematik und Mechanik*, 97(-):1–10, 2017b. doi: 10.1002/zamm.201700122.

M. Aßmus, K. Naumenko, and H. Altenbach. Subclasses of mechanical problems arising from the direct approach for homogeneous plates. In H. Altenbach, J. Chróścielewski, V.A. Eremeyev, and K. Wiśniewski, editors, *Recent Developments in the Theory of Shells*, volume 110 of *Advanced Structured Materials*, pages 1–20. Springer, Singapore, 2019. doi: 10.1007/978-3-030-17747-8.

E. Carrera. Theories and finite elements for multilayered, anisotropic, composite plates and shells. *Archives of Computational Methods in Engineering*, 9(2):87–140, 2002. doi: 10.1007/BF02736649.

E. Carrera. Theories and finite elements for multilayered plates and shells: A unified compact formulation with numerical assessment and benchmarking. *Archives of Computational Methods in Engineering*, 10(3):215–296, 2003. doi: 10.1007/BF02736224.

A.-L. Cauchy. *Recherches sur l'équilibre et le mouvement intérieur des corps solides ou fluides. élastiques ou non élastiques*, volume 2 of *Cambridge Library Collection - Mathematics*, pages 300–304. Cambridge University Press, 2009. doi: 10.1017/CBO9780511702518.038.

E. Cosserat and F. Cosserat. *Théorie des corps déformables*. A. Hermann et fils, Paris, 1909. URL http://jhir.library.jhu.edu/handle/1774.2/34209.

J. Eisenträger, K. Naumenko, H. Altenbach, and J. Meenen. A user-defined finite element for laminated glass panels and photovoltaic modules based on a layer-wise theory. *Composite Structures*, 133:265–277, 2015. ISSN 0263-8223. doi: 10.1016/j.compstruct.2015.07.049.

J.-F. Ganghoffer. *Cosserat, Eugène and François*, pages 1–6. Springer, Berlin, Heidelberg, 2017. doi: 10.1007/978-3-662-53605-6_49-1.

E. Hinton, D. R. J. Owen, and G. Krause. *Finite Elemente Programme für Platten und Schalen*. Berlin · Heidelberg, 1990. doi: 10.1007/978-3-642-50182-1.

R. Hooke. *Lectures de Potentia restitutiva, or of Spring explaining the power of springing bodies*. John Martyn, London, 1678. URL http://data.onb.ac.at/rep/103F4578.

G. R. Kirchhoff. Über das Gleichgewicht und die Bewegung einer elastischen Scheibe. *Journal für die reine und angewandte Mathematik*, 40:51–88, 1850. doi: 10.1515/crll.1850.40.51.

G. Lamé. *Leçons sur la théorie mathématique de l'elasticité des corps solides*. Gauthier-Villars, Paris, 1866.

A. Libai and J. G. Simmonds. Nonlinear elastic shell theory. *Advances in Applied Mechanics*, 23:271–371, 1983. doi: 10.1016/S0065-2156(08)70245-X.

R. D. Mindlin. Influence of rotatory inertia and shear on flexural motions of isotropic, elastic plates. *Journal of Applied Mechanics*, 18:31–38, 1951.

P. M. Naghdi. The Theory of Shells and Plates. In W. Flügge, editor, *Encyclopedia of Physics - Linear Theories of Elasticity and Thermoelasticity*, volume VI, a/2 (ed. C. Truesdell), pages 425–640. Springer, Berlin · New York, 1972. doi: 10.1007/978-3-662-39776-3_5.

K. Naumenko and V. A. Eremeyev. A layer-wise theory for laminated glass and photovoltaic panels. *Composite Structures*, 112: 283–291, 2014. doi: 10.1016/j.compstruct.2014.02.009.

W. Noll. A mathematical theory of the mechanical behavior of continuous media. *Archive for Rational Mechanics and Analysis*, 2(1):197–226, 1958. doi: 10.1007/BF00277929.

E. Oñate. *Structural Analysis with the Finite Element Method Linear Statics: Volume 2. Beams, Plates and Shells*. Springer, Dordrecht, 2013. doi: 10.1007/978-1-4020-8743-1_6.

J. Rychlewski. On Hooke's law. *Priklat. Mathem. Mekhan.*, 48(3):303–314, 1984. doi: 10.1016/0021-8928(84)90137-0.

J. C. Simo and D. D. Fox. On a stress resultant geometrically exact shell model. part i: Formulation and optimal parametrization. *Computer Methods in Applied Mechanics and Engineering*, 72(3):267–304, 1989. doi: 10.1016/0045-7825(89)90002-9.

J. C. Simo, D. D. Fox, and M. S. Rifai. On a stress resultant geometrically exact shell model. part ii: The linear theory; computational aspects. *Computer Methods in Applied Mechanics and Engineering*, 73(1):53–92, 1989. doi: 10.1016/0045-7825(89)90098-4.

B. Szabó and I. Babuška. *Finite Element Analysis*. John Wiley & Sons, Inc., New York · Chichester · Brisbane · Toronto · Singapore, 1991.

S. Vlachoutsis. Shear correction factors for plates and shells. *International Journal for Numerical Methods in Engineering*, 33 (7):1537–1552, 1992. doi: 10.1002/nme.1620330712.

W. Voigt. Über die Beziehung zwischen den beiden Elasticitätskonstanten isotroper Körper. *Wiedemann´sche Annalen*, 38: 573–587, 1889. doi: 10.1002/andp.18892741206.

P. A. Zhilin. Mechanics of deformable directed surfaces. *International Journal of Solids and Structures*, 12(9):635 – 648, 1976. doi: 10.1016/0020-7683(76)90010-X.